NACA RM A55A06

NACA

RESEARCH MEMORANDUM

SUMMARY OF THE FLIGHT CONDITIONS AND MANEUVERS IN WHICH MAXIMUM WING AND TAIL LOADS WERE EXPERIENCED ON A SWEPT-WING FIGHTER AIRPLANE

By Melvin Sadoff

Ames Aeronautical Laboratory
Moffett Field, Calif.

NATIONAL ADVISORY COMMITTEE
FOR AERONAUTICS

WASHINGTON

March 30, 1955

NATIONAL ADVISORY COMMITTEE FOR AERONAUTICS

RESEARCH MEMORANDUM

SUMMARY OF THE FLIGHT CONDITIONS AND MANEUVERS IN WHICH MAXIMUM WING AND TAIL LOADS WERE EXPERIENCED ON A SWEPT-WING FIGHTER AIRPLANE

By Melvin Sadoff

SUMMARY

Wing and tail-load data on a swept-wing fighter airplane were examined to determine the flight conditions and maneuvers in which maximum wing and tail loads were experienced, and, where pertinent, to relate these loads to the important stability and control changes that occurred. The results indicated that maximum wing loads and bending moments would be expected at relatively low Mach numbers. With increasing test Mach number, a relieving effect on the wing-panel loading coefficients was noted, apparently due to an increased tendency toward premature flow separation on the outboard wing sections. However, it was also indicated that the longitudinal instability or pitch-up, which results from premature tip separation, could lead to load factors and wing loads in excess of design values. Maximum horizontal-tail loads were experienced at Mach numbers less than about 0.95 during abrupt recoveries from pitch-ups. Fairly large balancing down loads were experienced at Mach numbers above about 0.95, even though low control power limited the load factors to values considerably below the design boundary. The largest vertical-tail loads were encountered in fishtail maneuvers at Mach numbers less than about 0.90. At Mach numbers above 0.95, relatively small vertical-tail loads were attainable due to low rudder control power.

Results are also presented on the use of controls in the various maneuvers for which loads data were obtained.

INTRODUCTION

The transonic stability and control characteristics of a swept-wing fighter airplane have been extensively investigated in flight (e.g., refs. 1 to 3). In the course of these investigations, information on horizontal- and vertical-tail loads was obtained for a wide range of flight maneuvers

and conditions. The horizontal-tail-load results have been presented in reference 4. In addition, the results of a separate series of tests (ref. 5) provided information on wing-panel load distribution at transonic speeds.

It is the purpose of this paper to summarize and examine these flight-loads data in order to identify the maneuvers and flight conditions wherein maximum wing and tail loads were experienced and, where pertinent, to relate these maximum loads to stability and control changes that occurred.

The loads data presented herein were obtained only at high altitude and, in the case of the horizontal- and vertical-tail loads, were incidental to the primary stability and control investigation; therefore, they do not necessarily represent the maximum loads that could be imposed on the airplane. However, it is felt that, in general, the wing and tail loads for the balancing condition (zero or small angular acceleration) were the maximum that could be imposed on this airplane at the test altitude.

SYMBOLS

b_p	wing-panel span (one side), ft
c	wing chord, ft
C.P.	lateral distance from wing-fuselage juncture to center of pressure of additional load on wing panel, $\frac{y_{C.P.}}{b_p}$
C_N	normal-force coefficient
C_{N_A}	airplane normal-force coefficient, $\frac{Wn}{qS}$
C_{N_p}	wing-panel normal-force coefficient, $\frac{2N_p}{qS}$
C_{n_p}	yawing-moment coefficient due to rolling velocity
C_{b_p}	wing-panel bending-moment coefficient, $C_{N_p} \times C.P.$
F_e	elevator stick force (pull force, positive), lb
F_a	aileron stick force (right force, positive), lb

[redacted]

h_p	pressure altitude, ft
i_t	stabilizer angle (trailing edge down, positive), deg
L_H	horizontal-tail normal load (up load, positive), lb
L_V	vertical-tail normal load (right load, positive), lb
M	Mach number
N_p	wing-panel additional normal load, lb
n	airplane normal load factor, $\frac{C_{N_A} qS}{W}$
$\frac{P}{2}$	time required to deflect, then return, control to trim position, sec
p	rolling velocity (right roll, positive), radians/sec
$\dot{p}$	rolling acceleration (right, positive), radians/sec^2
q	dynamic pressure, $\frac{\rho V^2}{2}$, lb/sq ft
r	yawing velocity (nose right, positive), radians/sec
$\dot{r}$	yawing acceleration (nose right, positive), radians/sec^2
S	wing area, sq ft
t	time, sec
V	airplane velocity, ft/sec
W	airplane weight, lb
$y_{C.P.}$	lateral distance from wing-fuselage juncture to wing-panel center of pressure of additional load, ft
β	sideslip angle (right sideslip, positive), deg
δ_e	elevator angle (down elevator, positive), deg
$\dot{\delta}_e$	elevator rate (down, positive), deg/sec
δ_{a_L}	left aileron angle (down aileron, positive), deg

[redacted]

δ_{a_R}	right aileron angle (down aileron, positive), deg
δ_{a_T}	total aileron angle ($\delta_{a_L} - \delta_{a_R}$)(stick right, positive), deg
$\dot{\delta}_{a_T}$	total aileron rate (stick right, positive), deg/sec
δ_r	rudder angle (right rudder, positive), deg
$\dot{\delta}_r$	rudder rate (right rudder, positive), deg/sec
$\dot{\theta}$	pitching velocity (nose up, positive), radians/sec
$\ddot{\theta}$	pitching acceleration (nose up, positive), radians/sec^2
ω_{δ_e}, ω_{δ_a}, ω_{δ_r}	control frequencies, $\frac{\pi}{P/2}$, radians/sec
ρ	air density, slugs/cu ft
Δ	before a symbol denotes change of that quantity from an initial or trim condition

Subscripts

max	maximum value
bal	balancing
$\ddot{\theta}$	pitching acceleration

TEST EQUIPMENT

The test airplane was a jet-powered fighter with sweptback wing and tail surfaces. A photograph and a two-view drawing of the airplane are presented in figures 1 and 2, respectively. The physical characteristics of the airplane are listed in table I.

Standard NACA instruments and multichannel oscillographs were used to record all measured quantities. The details of the strain-gage instrumentation used to measure horizontal-tail loads are described in reference 4. The instrumentation used to measure the wing-panel load

[redacted]

distribution is described in detail in reference 5. Airplane sideslip angle was measured by a vane mounted on the nose boom about 7 feet ahead of the nose inlet.

TEST CONDITIONS

The center of gravity of the test airplanes for these tests was located between 22.0 percent and 23.0 percent of the mean aerodynamic chord. The test weight of the airplanes, as flown, varied between 12,000 and 13,000 pounds. At Mach numbers up to about 0.96, the elevator was, in general, the primary longitudinal control with the stabilizer setting fixed at about 0.6°. Above 0.96 Mach number, the movable stabilizer was generally used to maneuver the airplane. The automatic wing leading-edge slats were locked in the closed position for the wing-panel loads tests and, though not locked, they remained closed over most of the lift-coefficient range covered in the tail-load tests. The nominal pressure altitude for these tests was 35,000 feet.

Wing-Panel Loads

The wing-panel load distribution was measured in gradually tightening turns, diving turns, and pull-outs at approximately constant Mach number. The range of Mach number and load factor reached in these tests is shown in figure 3. Also shown in this figure are the design Mach number load-factor envelope (based on a low-speed maximum-lift coefficient of 1.14) and the airplane buffet boundary to show the flight range above this boundary for which the wing-panel loads were determined.

Horizontal-Tail Loads

Horizontal-tail loads were measured over the Mach number and load-factor range shown in figure 4. The design Mach number load-factor envelope and the buffet boundary are also included in figure 4. Balancing loads were measured in gradually tightening turns, diving turns, and pull-outs. Maneuvering loads were obtained in abrupt recoveries from pitch-ups, in positive elevator-pulse maneuvers (abrupt push-downs), and in a few pull-up push-down maneuvers. The curve labeled n for $(L_{H_{bal}})_{max}$ in figure 4 defines the load factor at which the maximum positive or negative balancing loads on the horizontal tail were experienced. Below approximately 0.95 Mach number where the maximum balancing load is generally positive, the curve is different from the test-limits curve because the airplane (and wing-fuselage combination) tends to become stable

again after an initial instability or pitch-up. (See sketch below.)

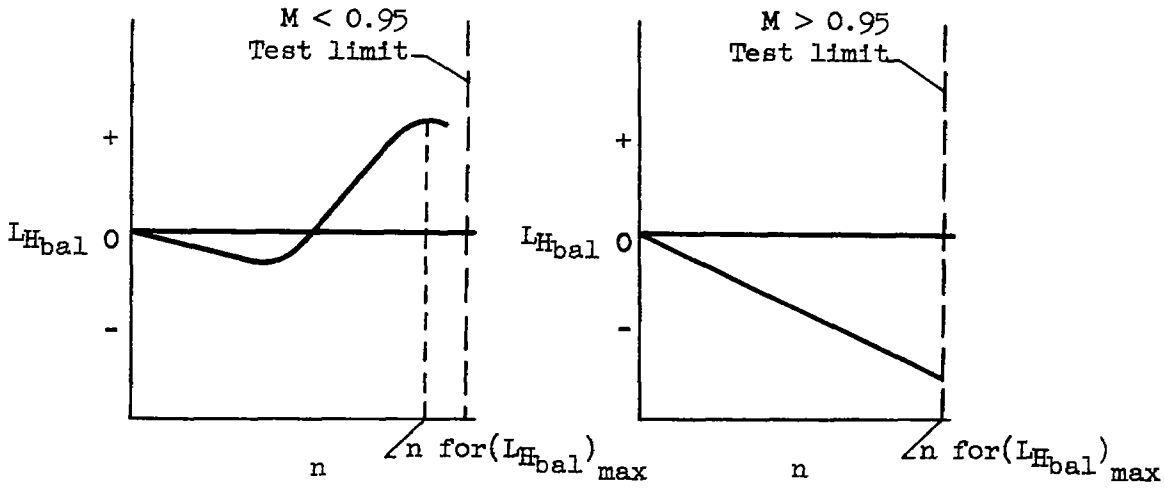

It should be noted that it was not possible to define accurately the tail-load variation much above the load-factor boundary for maximum positive balancing loads because of the difficulty of reducing the data obtained in this flight range.

Buffet loads were measured in the flight region between the buffet boundary and the positive test limits shown in figure 4.

Vertical-Tail Loads

Although vertical-tail loads were not directly measured in these tests, it was possible to derive them from the sideslip angles, rudder angles, and yawing accelerations measured in various type maneuvers. The maximum sideslip angles reached in steady sideslips, rudder pulses (abrupt rudder kicks), fishtail maneuvers, and rolling pull-out maneuvers are shown in figure 5 over a Mach number range of about 0.5 to 1.05.

RESULTS AND DISCUSSION

Wing-Panel Loads

The test-limits boundary obtained from reference 5 and reproduced in figure 3 shows that the design positive load factor was approached over most of the Mach number range. At the design diving speed, however, the maximum load factor attainable was only about one half the design value, due to control power limitations.

[redacted]

In figure 6, the main results from reference 5 of the wing-panel additional-load distribution tests are summarized. Figures 6(a) and 6(b) show, respectively, the variation of wing-panel normal-force coefficient and lateral position of the center of pressure of additional loading with Mach number at several values of airplane normal-force coefficient. The wing-panel bending-moment coefficient is shown in figure 6(c) as a function of Mach number at several values of airplane normal-force coefficient. The results in figures 6(a) and 6(c) indicate a fairly large relieving effect on the loading coefficients with increasing Mach number, so that at high subsonic speeds, the wing-panel normal-force and bending-moment coefficients are only about 70 percent and 65 percent, respectively, of their low subsonic-speed values. This relieving effect probably stems from an increased tendency for premature flow separation on the outboard wing sections at the higher Mach numbers, even at relatively low normal-force coefficients. It may also be seen in figure 6(c) that increasing normal-force coefficient, at constant Mach number, has a relieving effect on the bending-moment coefficients, since the ratio C_{b_p}/C_{N_A} decreases with increasing C_{N_A}. It may be concluded from these results that the maximum wing-panel bending moments would be experienced at a Mach number of 0.70 or less and at low altitude where the positive design load factor is attained at low normal-force coefficients. A comparison of the results in figure 6(b) with data for a 6-percent-thick 45° sweptback wing given in reference 6 indicates that wing thickness may be an important factor in determining the direction of the lateral center-of-pressure movement at transonic speeds.[1] Alleviating, inboard shifts of load occurred for the test airplane, while outboard movements of load were observed for the thin-wing results of reference 6.

Some information on the accuracy with which wing-panel loading may be predicted is provided in figure 7. The estimated results in figure 7(a) were based on Weissinger's lifting-surface theory as outlined in reference 7. The predicted results in figure 7(b) are based on the method described in reference 8. In computing the theoretical results in figures 7(a) and 7(b), no attempt was made to account for the influence of the fuselage on the span load distributions, since this effect is believed to be negligible for the test airplane. The comparison indicates a reasonable prediction of the flight loading at 0.7 Mach number and a conservative estimation at a Mach number of 1.0.

It has been shown that the wing-panel bending moments become less critical within the design load-factor envelope with increase in both Mach number and load factor due to premature tip stalling. However, the resulting decrease in static longitudinal stability (pitch-up) may result in wing loads and bending moments in excess of design values at low altitudes where the stall would not limit the load factors to values below that for design. The results in figure 8 show the variation of airplane normal-force coefficient with Mach number for the design load factor of 7.33 at pressure

[1]Sweepback may also be an important factor in determining the direction of movement of the lateral center of pressure at transonic speeds.

[redacted]

altitudes of 12,000, 25,000, and 35,000 feet. Also shown are the pitch-up boundary and the test limits reached at the test altitude. These data show that maneuvering at or near the pitch-up boundary between 12,000 and 25,000 feet may result in exceeding the design load factor and the design wing loads inadvertently.[2]

Horizontal-Tail Loads

The test-limits boundaries shown in figure 4 were reproduced from results originally presented in reference 4. These results show that tail loads were measured in maneuvers up to about the positive design load-factor envelope, except for Mach numbers greater than 0.90 where control power limitations reduced the maximum load factors to values considerably below that for design. The negative test limits shown were obtained in abrupt elevator push-down maneuvers.

The primary results on the maximum balancing, maneuvering, and buffeting horizontal-tail loads obtained within the test limits shown in figure 4 during the tests of reference 4 are summarized in figures 9(a), 9(b), and 9(c), respectively. The balancing loads reached a maximum positive value of about 1400 pounds at a Mach number of 0.80. The maximum balancing load, a down load of 2600 pounds, was experienced at a Mach number of 0.96. At higher Mach numbers, the balancing load decreased due to a reduction in the maximum load factor attainable.[3] The rapid change from moderate up loads to relatively high down loads at Mach numbers near 0.95 was due to an abrupt increase in wing-fuselage stability and a change in trim at the higher normal-force coefficients as the Mach number was increased through 0.95. These changes in stability and trim apparently result from both a rearward shift of chordwise loading and from the outboard wing sections maintaining unseparated flow to higher normal-force coefficients (ref. 5). A typical time history of a dive pull-out in the neighborhood of this transition flight region illustrating the effect of these changes on the tail-load variation at high subsonic speed is presented in figure 10. At Mach numbers above 0.95, a maximum down-load of about 2000 pounds was experienced at a load factor of about 4.5. As the Mach number decreased through 0.95, the tail load changed abruptly in a positive direction, reflecting the abrupt nose-up change in trim. This

[2]It should be noted that the probability of inadvertently exceeding the design load factor depends on a number of factors, among which are control power and pitching moment of inertia. The test airplane tends to be critical in these two respects, since it has a relatively low moment of inertia and, in the Mach number range where the pitch-up is most severe, the control effectiveness is low. These factors must be carefully examined when the loads aspects of pitch-up are assessed.

[3]Results in reference 4 indicate that if design load factor could be developed, a maximum balancing down load of about 3500 pounds would be experienced at a Mach number of about 0.96 at 35,000 feet.

change in trim is discussed in detail in reference 1 in connection with the pitch-up that occurs with decreasing Mach number on the test airplane.

The maximum maneuvering tail loads in these tests (fig. 9(b)) were experienced between 0.80 and 0.90 Mach number. The curve labeled "pitch-up recoveries" was based on recent pitch-up tests which resulted in somewhat greater negative pitching accelerations, and consequently greater maneuvering tail loads, than those reported in reference 4. Since tail buffeting made it difficult to reduce the tail-load data in the pitch-up region, the maneuvering load was determined by adding the pitching-acceleration load, from these recent tests, to the balancing load (fig. 9(a)), determined from the tests reported in reference 4. The peak pitching accelerations and the associated normal load factors used to define the peak maneuvering tail loads in pitch-up recoveries are given in a subsequent section of this report. It is of interest to note in a typical time history of a pitch-up maneuver (fig. 11) that the pilot, in attempting to reduce the overshoot in normal load factor, introduces a large maneuvering load increment on the horizontal tail. The peak tail load of about 3800 pounds shown in figure 11 comprises a balancing load of approximately 1400 pounds and a pitching-acceleration load of about 2400 pounds. These results indicate that the horizontal-tail loads attain fairly large values during pitch-up recoveries, and that this type of maneuver should be considered as a realistic design maneuver which may result in critical tail loads, particularly when performed at low altitude. The peak loads experienced in elevator-pulse maneuvers (abrupt push-downs) and the peak positive load obtained in a pull-up push-down maneuver are also shown in figure 9(b). Typical time histories descriptive of these maneuvers are presented in figures 12 and 13, respectively. Although the peak loads shown in figures 12 and 13 are relatively small, extrapolated results in reference 4 indicate that if these maneuvers are performed advertently or inadvertently at low altitude to high normal load factors, critical maneuvering tail loads may be experienced. The first-peak loads developed in the push-down maneuvers reached a maximum between 0.70 and 0.80 Mach number (fig. 9(b)), decreasing at higher Mach numbers due, primarily, to a decrease in control effectiveness. (See ref. 2.) The maximum second-peak load was experienced at a Mach number of about 0.90 during the recovery portion of the push-down maneuver. At Mach numbers higher than 0.90, the recovery load decreased rapidly due, primarily, to an increase in wing-fuselage stability which resulted in an alleviating balancing load (rather than a reinforcing load, as was the case at lower Mach numbers).

The buffeting loads shown in figure 9(c) (previously presented in ref. 4) reached maximum values of about ±600 pounds at relatively low Mach numbers, decreasing rapidly to relatively small values at Mach numbers above 0.95. It should be noted, however, that at Mach numbers above 0.95, the buffet region was penetrated to a lesser extent than at lower Mach numbers due to reduced maximum load factors available and to increased load factors for the onset of buffeting (fig. 4).

[redacted]

Division of Load Between Wing Panel, Fuselage, and Horizontal Tail

The percentages of the total airplane load carried by the wing panels, the fuselage, and the horizontal tail are given in figures 14(a) to 14(d) for airplane normal-force coefficients ranging from 0.2 to 0.8. The results for the wing panel were taken from a previous section of this report. The tail loads were obtained from reference 4. The fuselage loads were determined by subtracting the sum of the wing-panel and tail loads from the total loads (given by an accelerometer located near the airplane center of gravity). The results in figure 14 show that the wing panel carried the greatest percentage of the total load at the lowest Mach number of these tests. With increasing M, the contribution of the wing panel to the total lift generally decreased, reaching a minimum of about 59 percent of the total load at a Mach number of 0.94 and a normal-force coefficient of 0.6. The percentage of total load carried by the fuselage at the lowest test Mach number was somewhat less than the percentage of total wing area blanketed by the fuselage, which is 17.5 percent. In this connection, it should be pointed out that the data in figure 14(a), which indicate a small down-load on the fuselage at a Mach number of 0.70, appear to be in error, since for these conditions the fuselage would be at a positive angle of attack. (See ref. 5.) However, relatively small errors in determining the wing-panel and airplane normal-force coefficients could readily account for this apparent discrepancy. With increasing Mach number, the percentage of the total load carried by the fuselage increased rapidly to more than twice the blanketed wing area and about 70 percent of the wing-panel load at a Mach number of 0.94 and a normal-force coefficient of 0.6. These results indicate that at moderate values of C_{N_A}, prediction of the wing-panel contribution to the total lift based on the ratio of exposed to total wing area would be unconservative by about 5 to 10 percent at a Mach number of 0.70 and conservative by approximately 20 to 25 percent at a Mach number of 0.94. The horizontal-tail contribution to the total lift is fairly small, reaching a maximum of about 4-percent C_{N_A} at Mach numbers above 0.95 where maximum balancing tail loads were experienced.

Comparison of these data with results for another 35° swept-wing airplane presented in reference 9 indicates rather poor agreement. The percentage of total load carried by the wing panel of the reference airplane remained essentially invariant up to the limit test Mach number of 0.90, while the results of the present tests show an alleviating decrease with Mach number. It should be noted that the wing of the reference airplane has a somewhat lower aspect ratio and is comprised of considerably different sections than the wing of the present test airplane.

Vertical-Tail Loads

The maximum sideslip angles attained in various maneuvers (fig. 5) decreased rapidly from about 10° at the lowest test Mach number to approximately 1° at the highest test Mach number of 1.05. The largest sideslip angles were attained in fishtail maneuvers and in steady sideslips where maximum pilot effort was applied. The rolling pull-out results shown were obtained at load factors below the pitch-up boundary.[4] The low maximum sideslip angles at supersonic speed were the result of both a large decrease in rudder effectiveness (ref. 3) and of an increase in rudder hinge moments.

The vertical-tail loads associated with the limit sideslip angles given in figure 5 and the corresponding rudder angles given in a later section were derived from the vertical-tail and rudder-effectiveness results given in reference 3 and the manufacturer's low-speed wind-tunnel results on the directional stability of the airplane with tail off. The derived vertical-tail loads are presented in figures 15 and 16. The maximum balancing loads obtained over the test Mach number range from the steady sideslip maneuvers are given in figure 15. Maximum rudder and stabilizer loads of approximately 2000 and 3000 pounds, respectively, are indicated at a Mach number of 0.80. At higher Mach numbers, a rapid decrease in load occurs due to a rapid loss in rudder control power. The total loads are small, generally remaining under 1000 pounds over the test Mach number range. The derived maximum maneuvering vertical-tail loads in rudder-pulse, fishtail, and rolling pull-out maneuvers are shown in figure 16. (Typical time histories of a rudder-pulse and a fishtail maneuver are shown in figs. 17 and 18, respectively.) In the case of the rudder-pulse loads, the first-peak load (which corresponds to the initial rudder deflection and occurs before appreciable sideslip has developed) was calculated considering that the load was that necessary to produce the first-peak yawing acceleration. The second-peak load (which corresponds to the abrupt return of the rudder to trim at or near maximum sideslip) was determined by adding the second-peak yawing-acceleration load to the balancing load (fig. 17). The peak loads in the rudder-pulse maneuvers attained maximum values between 0.70 and 0.80 Mach number (fig. 16). The maximum maneuvering load of about 3500 pounds was attained in a fishtail maneuver at a Mach number of about 0.70. The reason for the relatively large loads experienced in fishtail maneuvers may be seen in the time history of figure 18 where it is observed that the ratio of the

[4]Several rolling pull-out maneuvers were also performed above the pitch-up boundary between Mach numbers of 0.85 and 0.90. Although the pilot noted that these maneuvers were not practical and would not be performed advertently, the data obtained are considered of interest. Unfortunately, the sideslip records for these maneuvers are unavailable due to an instrument malfunction. No attempt was made subsequently to duplicate these maneuvers because they were unusually severe. The results that were obtained are discussed in a later section.

maximum sideslip angle developed per degree maximum rudder deflection, β/δ_r, at a Mach number of 0.8 is about 2.5, whereas in steady sideslips the ratio is only about 0.4. The β/δ_r ratios determined from the frequency-response tests of reference 3 and from the fishtail and steady-sideslip maneuvers of the present tests are presented in figure 19. Above about 0.80 Mach number, the results from the fishtail and frequency-response tests are in good agreement. At the lower Mach numbers, the values of β/δ_r obtained from the fishtail maneuvers are considerably below those obtained in the frequency-response tests, possibly because the pilot found it difficult to coordinate his rudder-pedal movements properly at the lower airplane natural frequencies. The values of β/δ_r measured in gradual sideslips are small, generally attaining only one fifth the values measured in fishtail maneuvers. The maximum load developed in a rolling pull-out maneuver, performed below the pitch-up boundary, was about 2500 pounds at a Mach number of 0.73. (See fig. 16.) A time history of this maneuver is presented in figure 20.

The rapid decrease in the maneuvering vertical-tail loads above a Mach number of about 0.85 (fig. 16) results from a rapid decrease in rudder and aileron control power that generally occurs at transonic speeds. (See ref. 3.)

The maximum load from these tests is only about one third of the design load based on 5° sideslip at limit diving speed at an altitude of 12,000 feet, indicating that this design requirement may be unduly conservative. However, in rolling pull-out maneuvers performed above the pitch-up boundary, the resulting violent airplane motions indicated that higher sideslip angles than those normally attained in other maneuvers might be experienced. A time history of a maneuver of this type is shown in figure 21. The pilot observed that the rolling motion shown in this figure felt like a succession of snap rolls and that he could not stop the roll until the airplane slowed to less than 0.70 Mach number from an initial Mach number of 0.90. Although the sideslip angle records were not available for this maneuver, a rough estimate of the sideslip developed during the maneuver of figure 21, using the relationships developed in reference 10,[5] indicated a value of about 10° at a Mach number of 0.84, and a tail load approximately one half the maximum design value. From the several rolling pull-out maneuvers performed in the pitch-up flight region, it appeared the violence of the maneuver depended on the initial aileron deflection - the smaller the deflection the less severe the maneuver. In the pilot's opinion this type maneuver was not a useful one and would not be performed advertently.

[5]Fairly good correlation has been found between the measured sideslip angles developed in rolling pull-outs below the pitch-up (fig. 5) and values estimated using the method described in reference 10. In the present case, values of C_{n_p} were estimated for the appropriate Mach number and normal-force coefficient rather than using a value of $C_{N_A}/16$ as suggested in reference 10.

[redacted]

Use of Controls in Longitudinal, Directional, and Lateral Maneuvers

The maximum elevator angles, rates, frequencies, and forces used in the various longitudinal maneuvers for which loads data were presented are shown in figure 22. The range of the maximum elevator angles used in gradual turns at normal accelerations from zero to the pitch-up boundary, and the maximum values used in elevator-pulse maneuvers and during recoveries from pitch-ups are shown in figure 22(a). These results show that about 50 percent of the available up-elevator deflection of 37° and 100 percent of the available down-elevator deflection of 17.5° were used in these longitudinal maneuvers. The maximum elevator rates used in the elevator-pulse maneuvers and in abrupt recoveries from pitch-ups are given in figure 22(b), where it may be seen that the highest rate of 180° per second was attained in an elevator-pulse maneuver. The maximum elevator frequencies used in the elevator-pulse maneuvers are presented in figure 22(c). The maximum elevator stick forces used in various maneuvers are given in figure 22(d). The stick forces labeled "elevator pulse" refer to the maximum required to deflect the elevator to the values shown in figure 22(a). A maximum pull force of 150 pounds was used during a dive pull-out at a Mach number of about 0.97.

The maximum pitching accelerations developed during elevator-pulse and pitch-up maneuvers are presented in figures 23(a) and 23(b) as functions of Mach number and normal load factor, respectively. The maximum negative acceleration reached in the pulse maneuvers of about -1.8 radians per second per second corresponds to the maximum first-peak load shown in figure 9(b) at a Mach number of 0.80. The maximum pitching acceleration of about -3.2 radians per second per second was reached during recovery from a pitch-up at a Mach number of 0.90 and a load factor of about 5. The relatively large negative pitching accelerations shown at a Mach number of about 0.90 in figure 23(a) result from the pilot's applying fairly large and abrupt corrective control deflections during pitch-up recoveries. (See figs. 22(a) and 22(b).) The peak negative pitching accelerations developed in elevator-pulse maneuvers at the highest test Mach number decreased to about one third the maximum subsonic-speed value due to the large decrease in elevator effectiveness that occurs at transonic speeds. From the results in figure 23(b), it appears the peak pitching accelerations developed either in recoveries from abrupt push-downs or in abrupt recoveries from pitch-ups are roughly proportional to the corresponding maximum normal load factors. An extrapolation of these results to the design positive and negative load factors gives values of pitching acceleration of about -5.0 and +2.5 radians per second per second. Comparison of these results with data in reference 11 obtained during operational training flights with several fighter airplanes (including the test airplane type) shows that the maximum elevator rates and pitching accelerations of these tests (figs. 22(b) and 23) were 50 to 100 percent greater than those recorded in the tests of reference 11. The maximum

rates of these tests, however, were obtained in elevator-pulse maneuvers which were made as abruptly as possible.[6] The considerably higher pitching accelerations obtained with the test airplane resulted from maneuvering at load factors above the pitch-up boundary. Most of the airplanes reported on in reference 11 were straight-wing types which do not experience pitch-up. The one swept-wing type, for which data were available, was restricted at high speeds to load factors below the buffet and pitch-up boundaries.

The maximum rudder angles, rates, and frequencies used in various directional maneuvers for which loads data were presented are given in figure 24. The maximum rudder angles used in steady sideslips, fishtail, and rudder-pulse maneuvers are shown in figure 24(a). These results indicate that about 60 percent of the available rudder deflection of ±28° was used in these directional maneuvers. The maximum rudder rates used in rudder-pulse and fishtail maneuvers are given in figure 24(b), where it is shown that the highest rate used was about 120° per second in a rudder-pulse maneuver. The maximum rudder frequencies used in the rudder-pulse maneuvers are shown in figure 24(c). The rudder-pedal forces were not measured during these tests. The maximum yawing accelerations developed in various type maneuvers are presented in figures 25(a) and 25(b) as functions of Mach number and sideslip angle, respectively. The maximum yawing acceleration of about 3 radians per second per second was obtained in a rolling pull-out maneuver at load factors above the pitch-up boundary. These maneuvers were, in general, very violent and virtually uncontrollable, and they would not ordinarily be performed advertently by the pilots. The maximum yawing acceleration recorded in the other maneuvers was about ±1.8 radians per second per second. The peak yawing accelerations developed in the rudder-pulse maneuvers at low supersonic speeds decreased to about one half the maximum subsonic speed value due to a rapid decrease in rudder effectiveness at transonic speeds.

It should be noted in connection with the data presented in figure 25 that sideslip angles were not available for the rolling pull-out points shown. Also, the yawing accelerations presented for the fishtail maneuvers were estimated from a flight-determined curve of r/δ_r as a function of Mach number, since they were not measured during the same flight the sideslip angles were measured.

The maximum aileron angles, rates, frequencies, and forces used in various lateral maneuvers are shown in figure 26. Total aileron deflections (fig. 26(a)) approached the maximum available of 28° in rudder-fixed aileron rolls, while the maximum aileron rates used were of the order of 120° per second (fig. 26(b)). The maximum aileron control frequency, as measured in aileron-pulse maneuvers (fig. 26(c)), was about 8 radians per second, and the control forces were moderate, reaching a maximum of about

[6]The test airplane was not equipped with a rate restrictor which limits the maximum elevator rates on most F-86A airplanes to about 45° per second.

[redacted]

60 pounds in a rolling pull-out maneuver at a Mach number of 0.87 (fig. 26(d)). Maximum rolling velocities and rolling accelerations developed in various maneuvers are shown in figures 27(a) and 27(b), respectively. The peak rolling velocity of about 4 radians per second was reached in a rolling pull-out maneuver at load factors above the pitch-up boundary. (See fig. 21.) The peak rolling acceleration of 8 radians per second per second was recorded in an abrupt aileron reversal maneuver at a Mach number of about 0.83. At Mach numbers above 0.90 both the peak rolling velocities and accelerations decreased abruptly to about one fourth of the maximum values attained at lower speed due to a rapid decrease in aileron effectiveness. (See ref. 3.)

CONCLUSIONS

Loads data obtained during extensive flight tests of a swept-wing airplane have been examined to define the flight conditions and maneuvers in which maximum wing and tail loads were experienced and to relate these maximum loads to the important stability and control changes that occurred. This examination has led to the following conclusions:

1. Maximum wing-panel loading coefficients were experienced at the lowest Mach number of these tests. Both increasing Mach number and normal-force coefficient had an alleviating effect on the wing-panel bending-moment coefficients due to premature tip separation and the resulting inboard shift of the lateral center of pressure. However, it was indicated that the associated longitudinal instability or pitch-up, which tends to be critical for the test airplane because of relatively low inertia and control power, could result in load factors and over-all wing loads in excess of design values.

2. Maximum horizontal-tail loads were encountered during abrupt recoveries from pitch-ups at Mach numbers less than 0.95. At Mach numbers greater than 0.95, the peak maneuvering loads decreased rapidly and the balancing loads became more critical due to an abrupt increase in wing-fuselage stability and changes in trim at the higher values of load factor. Control-power limitations resulted in lower peak values of load factor and, consequently, balancing down loads, at Mach numbers above 0.96.

3. Prediction of the wing-panel contribution to the total lift at moderate values of C_{N_A} based on the ratio of exposed to total wing areas would be unconservative by approximately 5 to 10 percent at a Mach number of 0.70 and conservative by about 20 to 25 percent at a Mach number of 0.94.

4. The largest vertical-tail loads of these tests were obtained in fishtail maneuvers at Mach numbers below 0.90. These loads were only

about one third the design load based on the 5° sideslip requirement at limit diving speed. At Mach numbers above about 0.90, the peak loads, developed in the various directional and lateral maneuvers, decreased rapidly due to a large reduction in rudder and aileron control power.

Ames Aeronautical Laboratory
National Advisory Committee for Aeronautics
Moffett Field, Calif., Jan. 6, 1955

REFERENCES

1. Anderson, Seth B., and Bray, Richard S.: A Flight Evaluation of the Longitudinal Stability Characteristics Associated with the Pitch-Up of a Swept-Wing Airplane in Maneuvering Flight at Transonic Speeds. NACA RM A51I12, 1951.

2. Triplett, William C., and Smith, G. Allan: Longitudinal Frequency-Response Characteristics of a 35° Swept-Wing Airplane as Determined from Flight Measurements, Including a Method for the Evaluation of Transfer Functions. NACA RM A51G27, 1951.

3. Triplett, William C., and Brown, Stuart C.: Lateral and Directional Dynamic-Response Characteristics of a 35° Swept-Wing Airplane as Determined from Flight Measurements. NACA RM A52I17, 1952.

4. Sadoff, Melvin: Flight Measurements of the Horizontal-Tail Loads on a Swept-Wing Fighter Airplane at Transonic Speeds. NACA RM A53G10, 1953.

5. Rolls, L. Stewart, and Matteson, Frederick H.: Wing-Load Distribution on a Swept-Wing Airplane in Flight at Mach Numbers Up to 1.11, and Comparison with Theory. NACA RM A52A31, 1952.

6. Loving, Donald L., and Williams, Claude V.: Aerodynamic Loading Characteristics of a Wing-Fuselage Combination Having a Wing of 45° Sweepback Measured in the Langley 8-Foot Transonic Tunnel. NACA RM L52B27, 1952.

7. DeYoung, John, and Harper, Charles W.: Theoretical Symmetric Span Loading at Subsonic Speeds for Wings Having Arbitrary Plan Form. NACA Rep. 921, 1948.

8. Cohen, Doris: Formulas for the Supersonic Loading, Lift and Drag of Flat Swept-Back Wings with Leading Edges Behind the Mach Lines. NACA Rep. 1050, 1951.

[redacted]

9. Mayer, John P., and Gillis, Clarence L.: Division of Load Among the Wing, Fuselage, and Tail of Aircraft. NACA RM L51E14a, 1951.

10. White, Maurice D., Lomax, Harvard, and Turner, Howard L.: Sideslip Angles and Vertical-Tail Loads in Rolling Pull-Out Maneuvers. NACA TN 1122, 1947.

11. Mayer, John P., Hamer, Harold A., and Huss, Carl R.: A Study of the Use of Controls and the Resulting Airplane Response During Service Training Operations of Four Jet Fighter Airplanes. NACA RM L53L28, 1954.

[redacted]

TABLE I.- PHYSICAL CHARACTERISTICS OF TEST AIRPLANE

Wing	
Total wing area (including flaps, slats, and 49.92 sq ft covered by fuselage), sq ft	287.90
Span, ft	37.12
Aspect ratio	4.79
Taper ratio	0.51
Mean aerodynamic chord (wing station 98.7 in.), ft	8.08
Dihedral angle, deg	3.0
Sweepback of 0.25-chord line, deg	34.23
Incidence of root chord, deg	1.0
Incidence of tip chord, deg	-1.0
Root airfoil section (normal to 0.25-chord line)	NACA 0012-64 (modified)
Tip airfoil section (normal to 0.25-chord line)	NACA 0011-64 (modified)
Ailerons	
Total area, sq ft	37.20
Span (one), ft	9.18
Chord (av.), ft	2.03
Maximum total aileron deflection, deg	±30
Fuselage	
Length, ft	34.04
Maximum diameter, ft	5.0
Fineness ratio	6.8
Horizontal tail	
Total area (including 1.20 sq ft covered by vertical tail), sq ft	34.99
Span, ft	12.8
Aspect ratio	4.65
Taper ratio	0.45
Mean aerodynamic chord (horizontal-tail station 33.54 in.), ft	2.89
Dihedral angle, deg	10.0
Sweepback of 0.25-chord line, deg	34.58
Airfoil section (parallel to center line	NACA 0010-64
Maximum stabilizer deflection, deg	1 nose up, 10 nose down
Horizontal-tail length, ft	18.25
Elevators	
Total area (including tabs and expanding balance area forward of hinge line), sq ft	10.1
Span (each), ft	5.8
Maximum elevator deflection, deg	37 up, 17.5 down
Boost	hydraulic

[redacted]

TABLE I.- PHYSICAL CHARACTERISTICS OF TEST AIRPLANE - Concluded

Vertical tail	
Total area (including 7.24 sq ft blanketed by fuselage and excluding 3.96 sq ft dorsal fin), sq ft	39.75
Span, ft	8.38
Aspect ratio	1.77
Taper ratio	0.345
Mean aerodynamic chord (vertical-tail station 42.9 in.), ft	4.90
Sweepback of 0.25-chord line, deg	35.0
Airfoil section (parallel to center line)	NACA 0011(10)-64
Vertical-tail length, ft	16.75
Rudder	
Area (including tab and excluding rudder balance forward of hinge line), sq ft	8.12
Span, ft	6.6
Maximum deflection, deg	±28
Boost	None
Average airplane weight, lb	12,400
Pitching moment of inertia, slug-ft^2	17,480
Yawing moment of inertia, slug-ft^2	23,200
Rolling moment of inertia, slug-ft^2	7,200

[redacted]

[redacted]

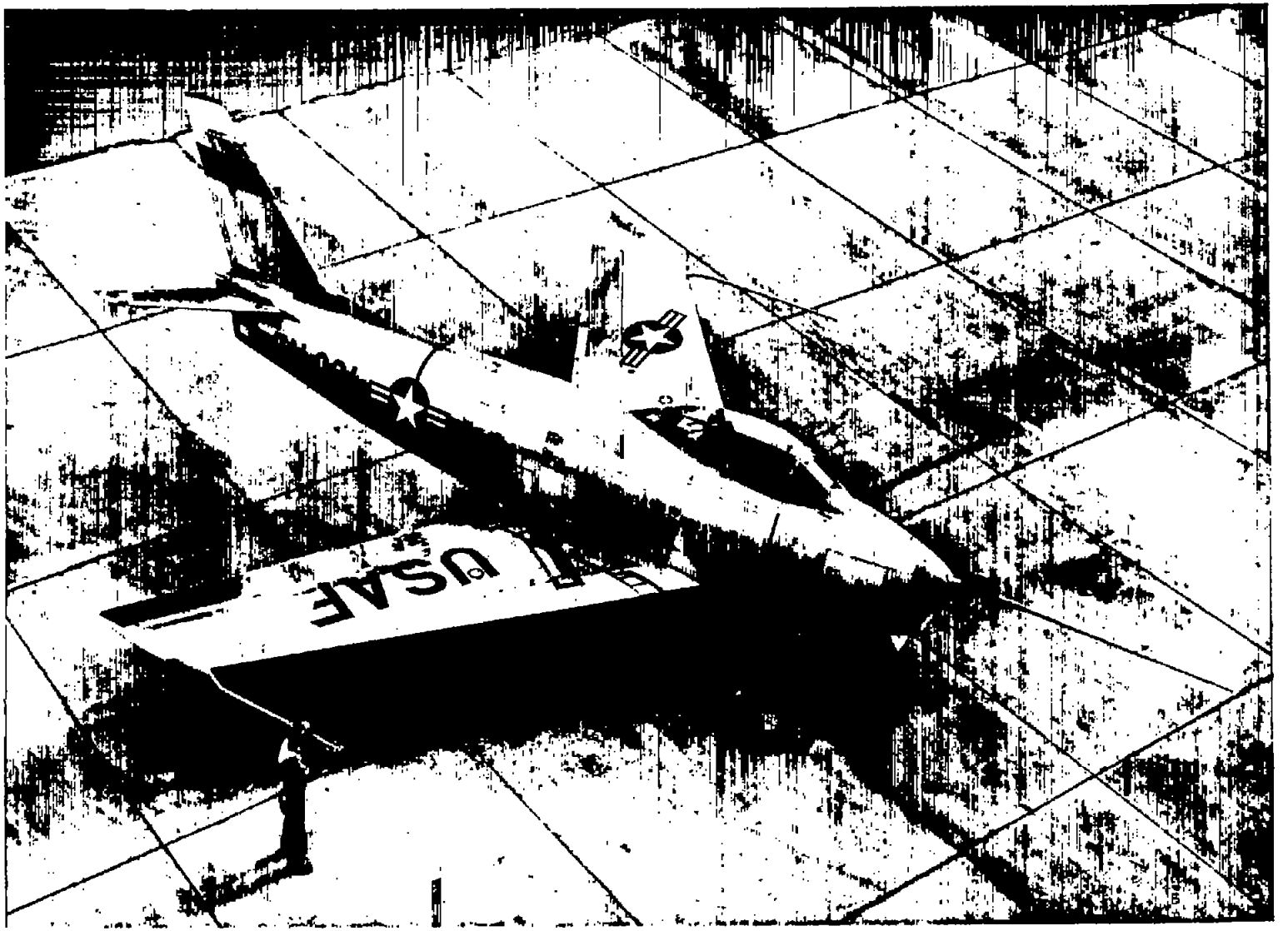

A-15004

Figure 1.- Photograph of the test airplane.

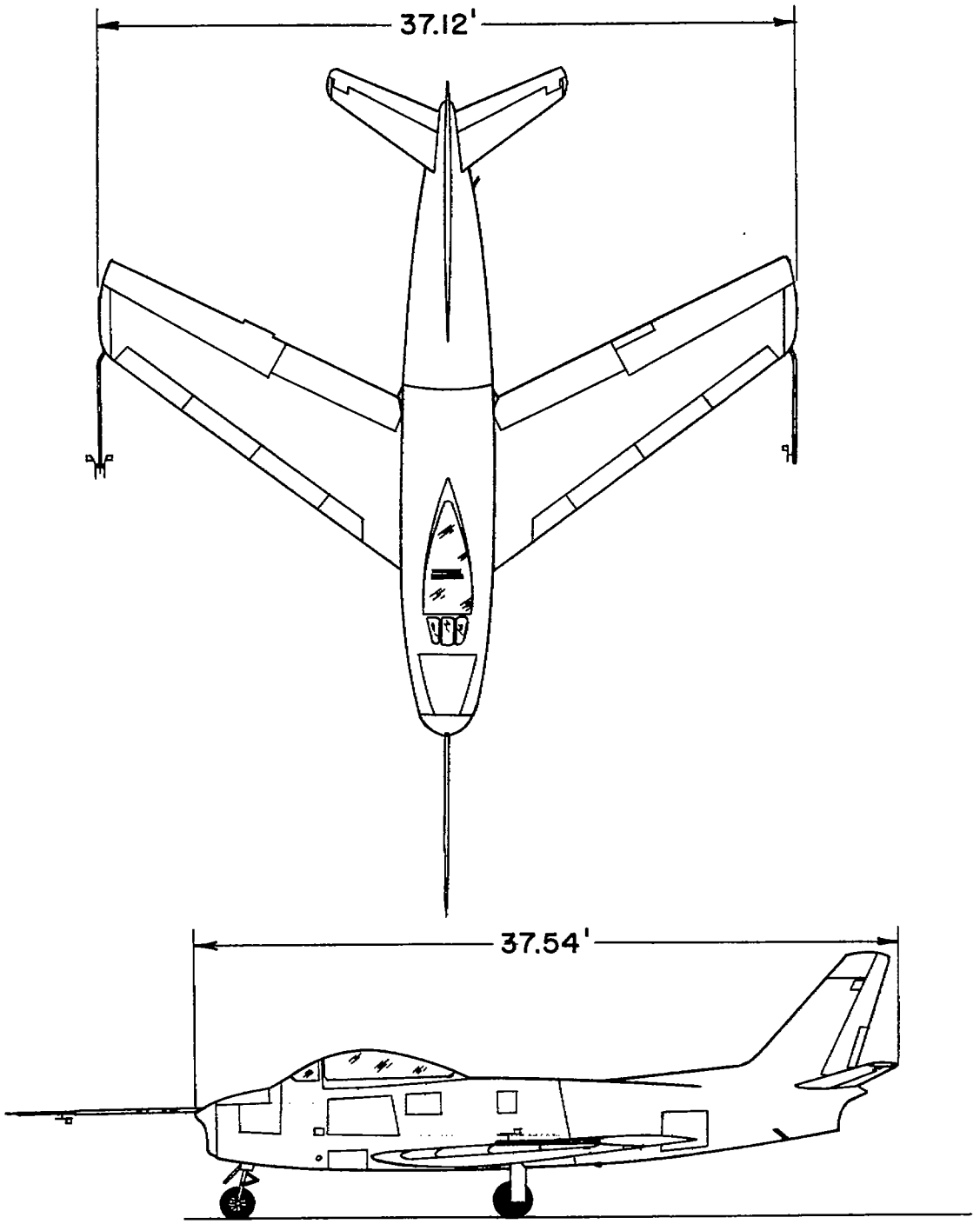

Figure 2.- Two-view drawing of the test airplane.

[redacted]

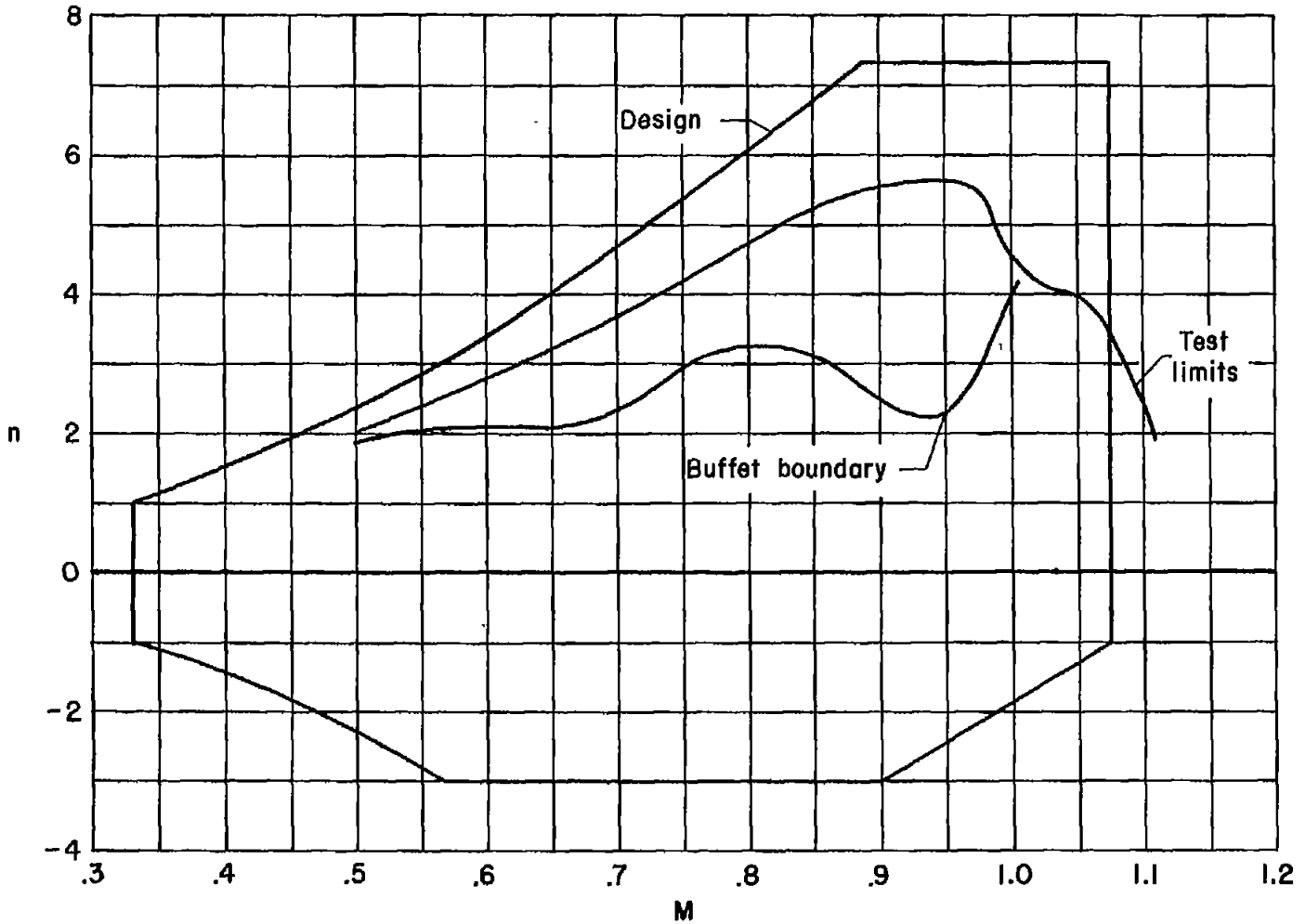

Figure 3.- Maximum load factors attained in wing load-distribution tests; pressure altitude, 35,000 feet.

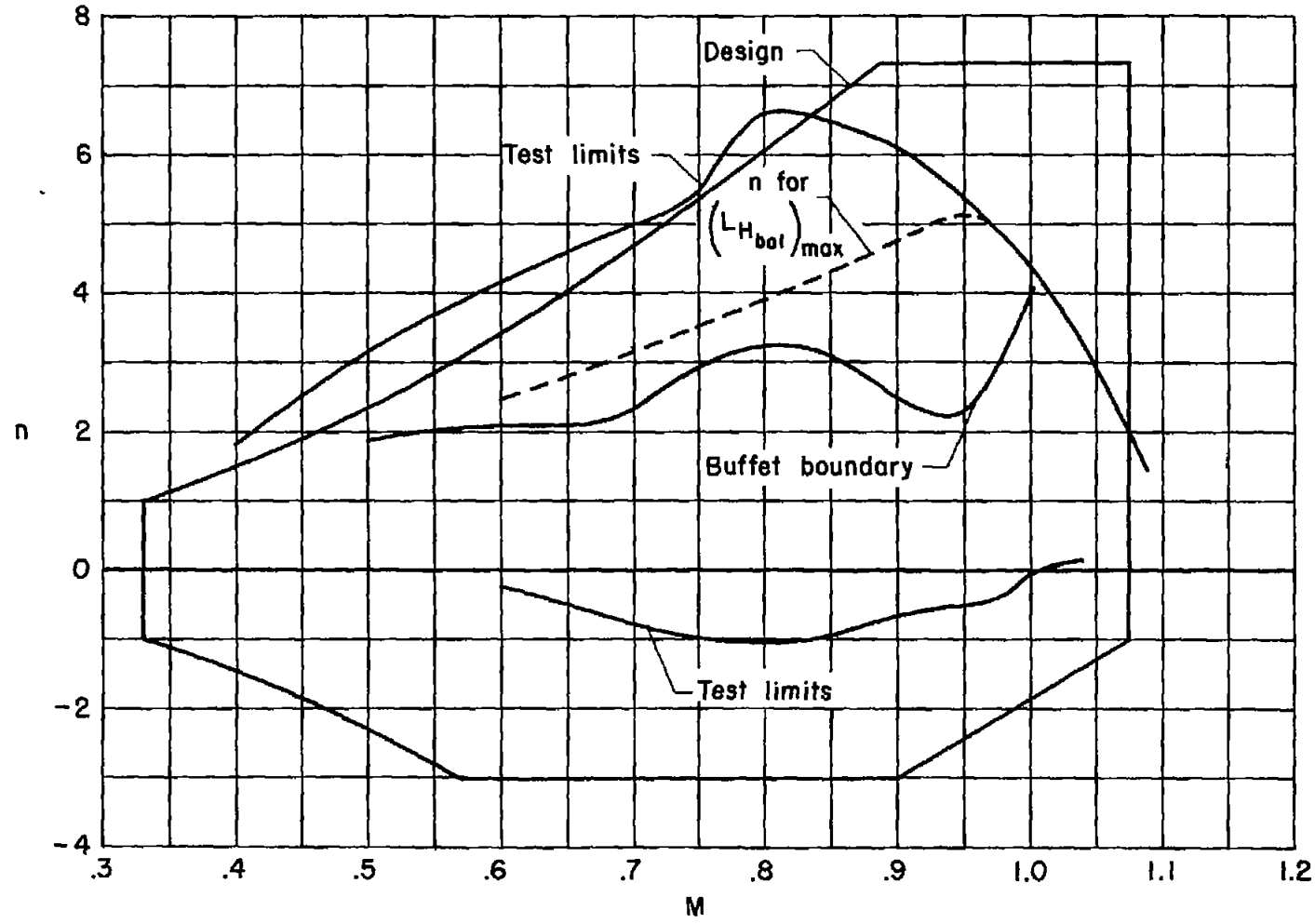

Figure 4.- Maximum load factors attained in horizontal-tail load tests; pressure altitude, 35,000 feet.

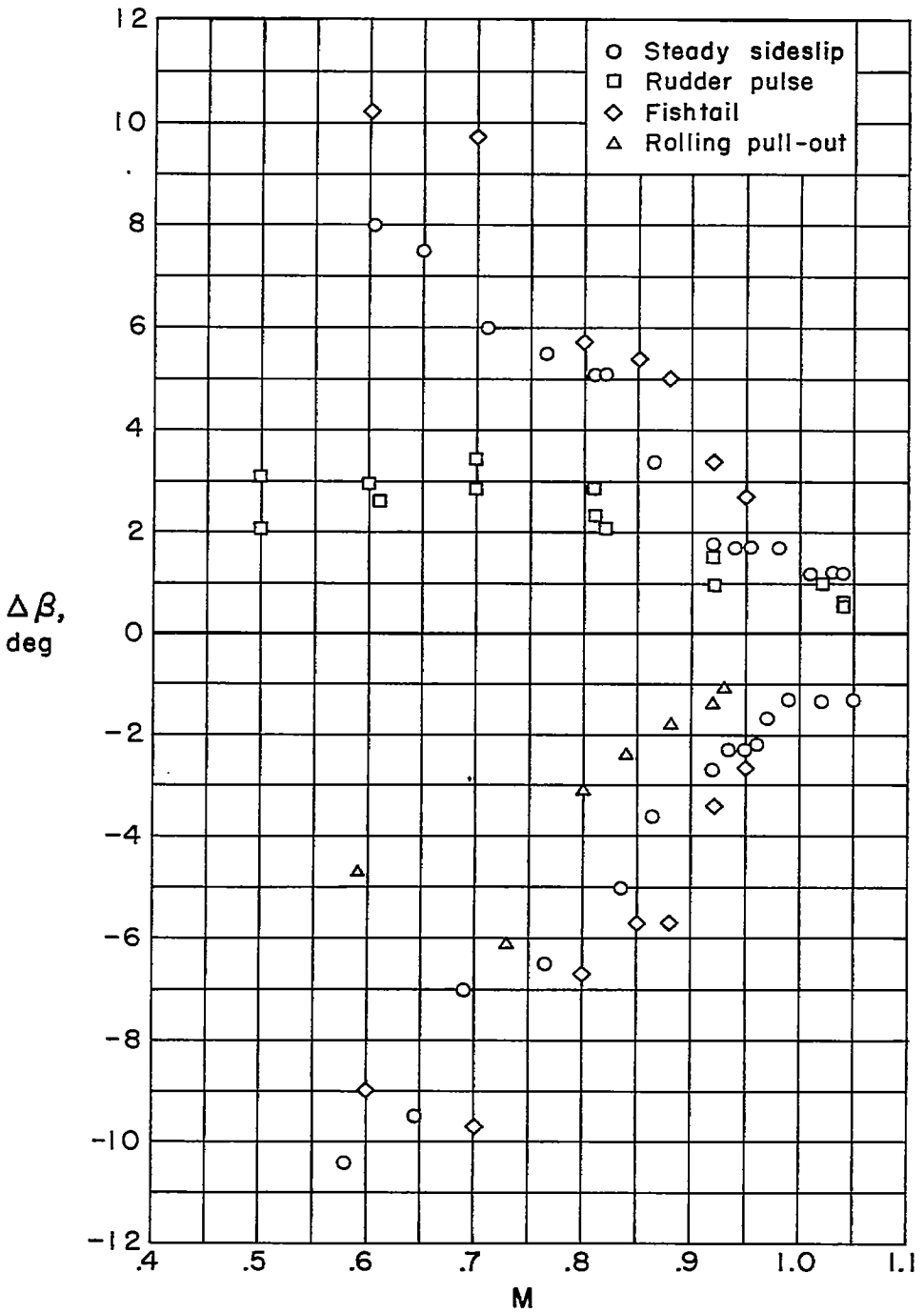

Figure 5.- Maximum sideslip angles attained in various directional and lateral maneuvers; pressure altitude, 35,000 feet.

[redacted]

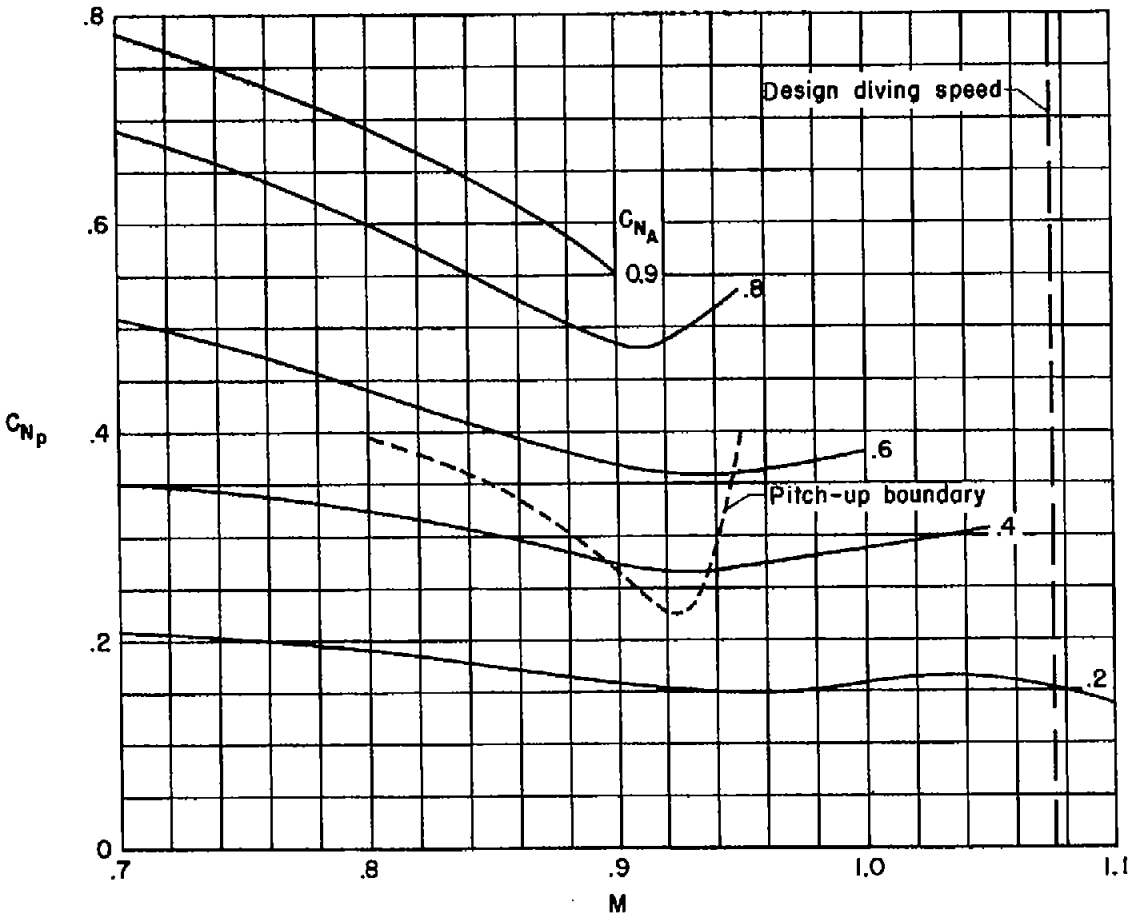

(a) Wing-panel normal-force coefficient.

Figure 6.- Variation of wing-panel normal-force coefficient, lateral position of the center of pressure and bending-moment coefficient with Mach number at several values of airplane normal-force coefficient; pressure altitude, 35,000 feet.

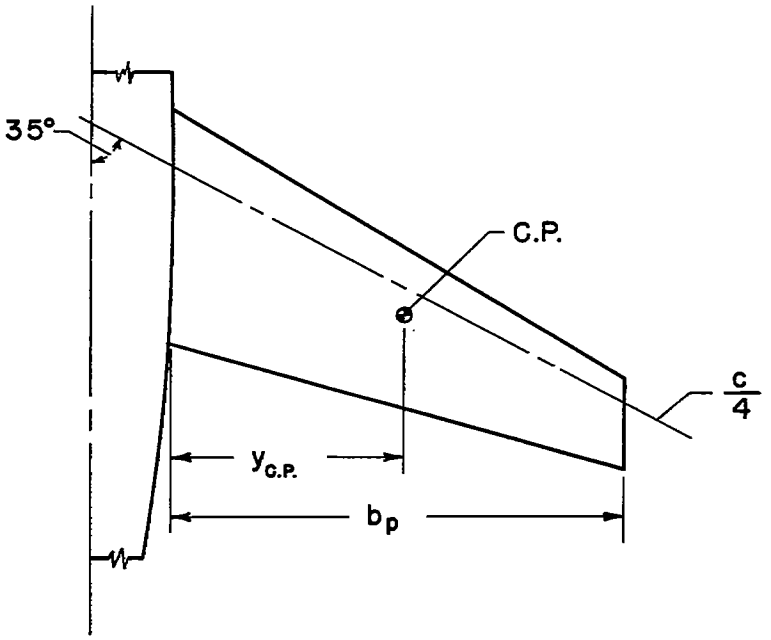

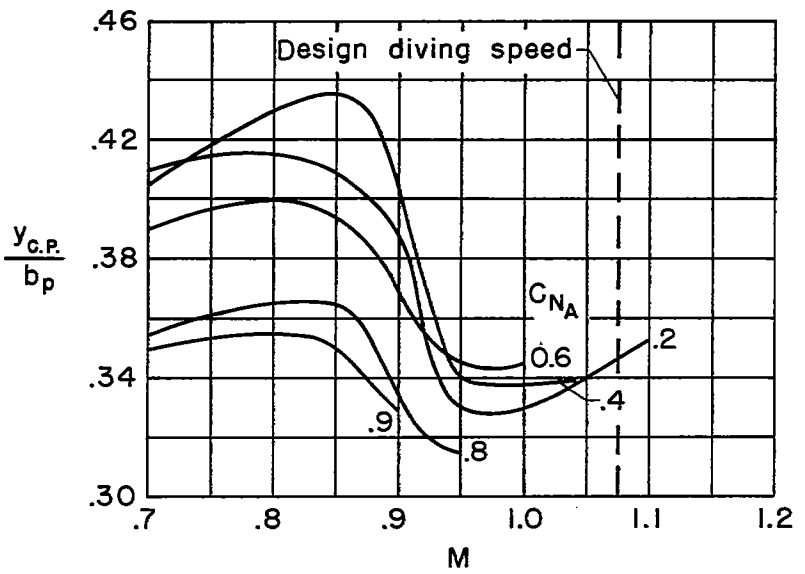

(b) Lateral center-of-pressure position.

Figure 6.- Continued.

[redacted]

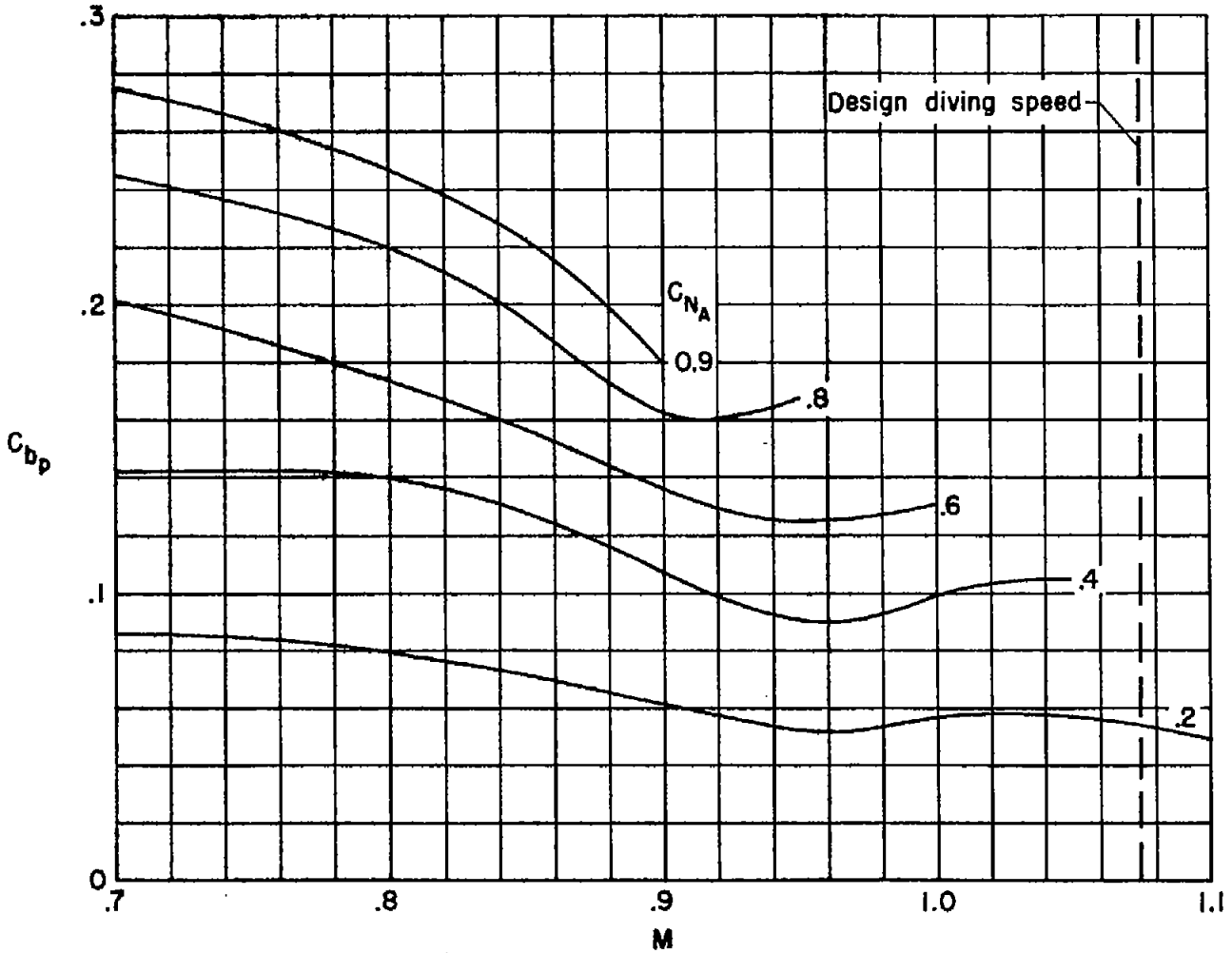

(c) Wing-panel bending-moment coefficient.

Figure 6.- Concluded.

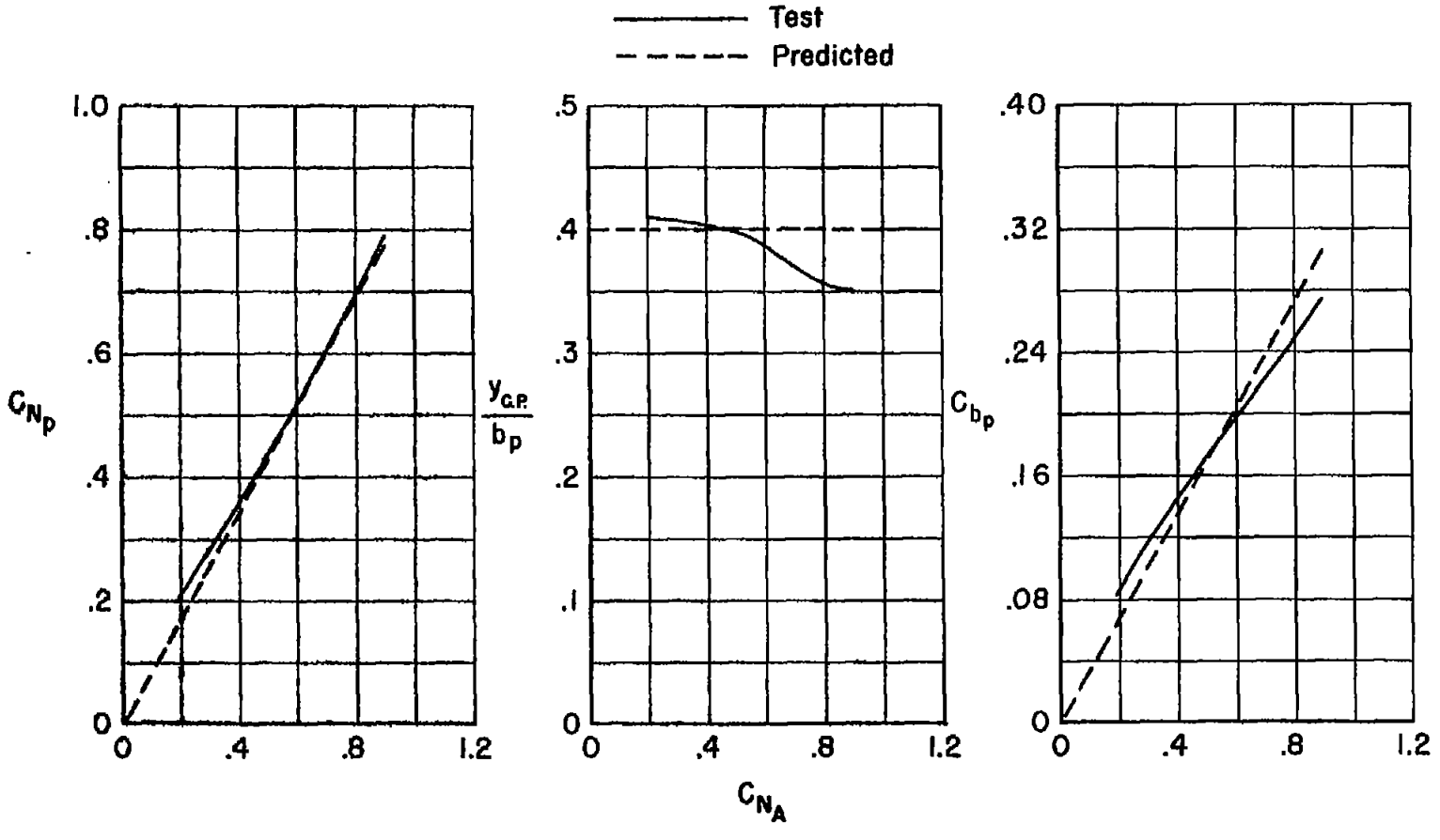

(a) M ≈ 0.70

Figure 7.- Comparison between the test results and predicted values of wing-panel normal-force coefficient, lateral position of the center of pressure, and bending-moment coefficient, at Mach numbers of approximately 0.70 and 1.0; pressure altitude, 35,000 feet.

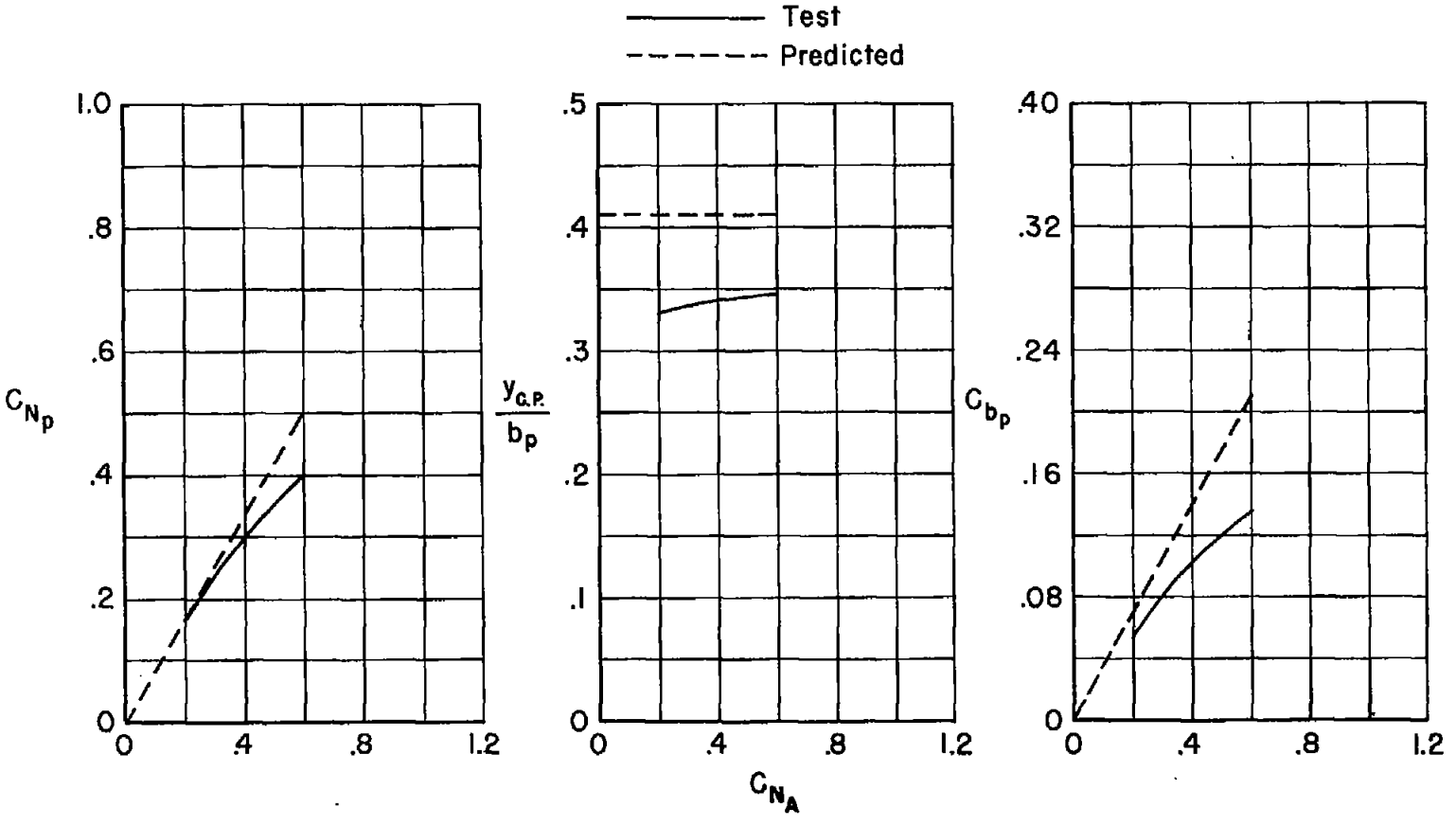

(b) M ≈ 1.0

Figure 7.- Concluded.

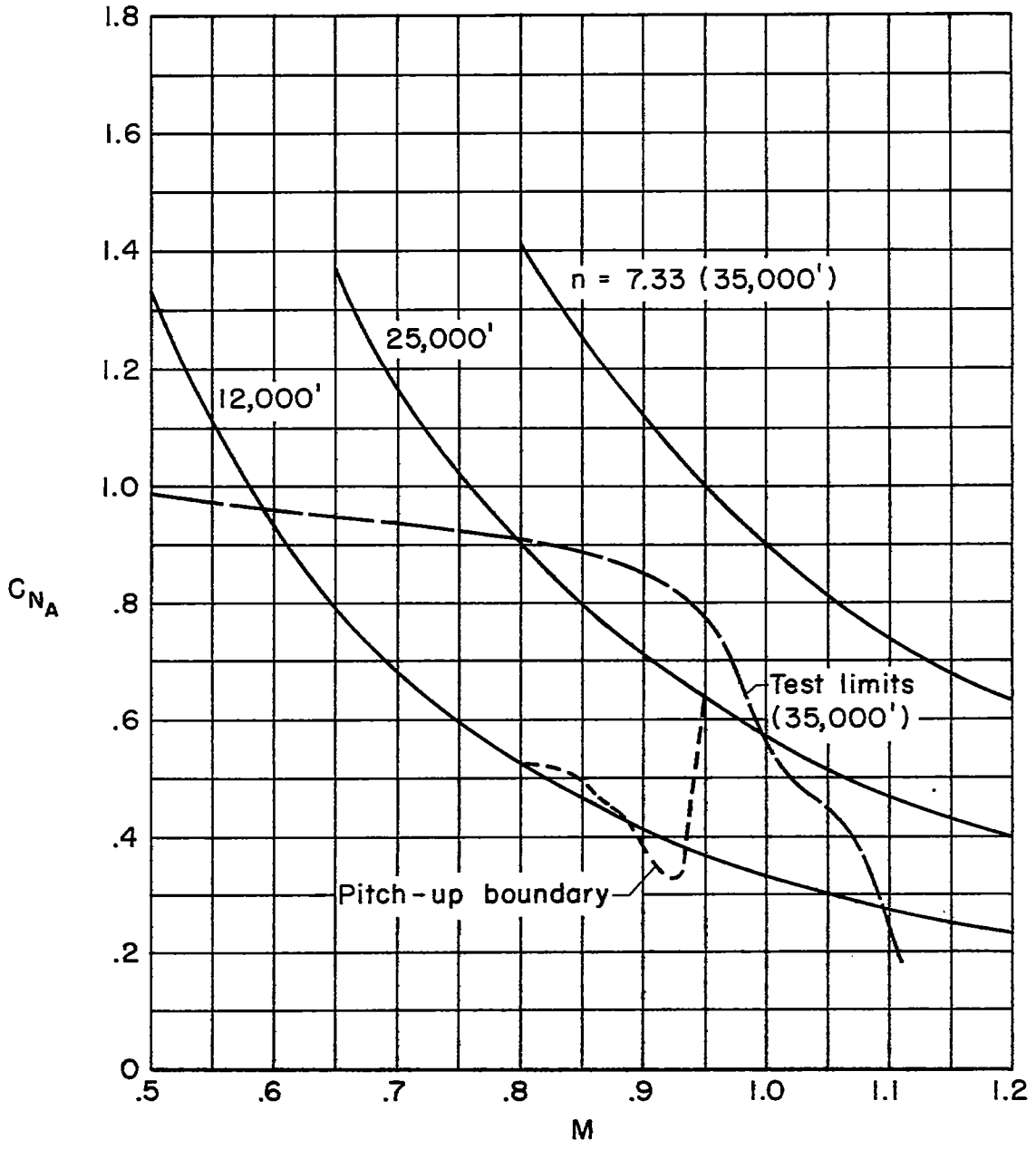

Figure 8.- Variation with Mach number of the airplane normal-force coefficient for the design load factor of 7.33 at altitudes of 12,000, 25,000, and 35,000 feet.

[redacted]

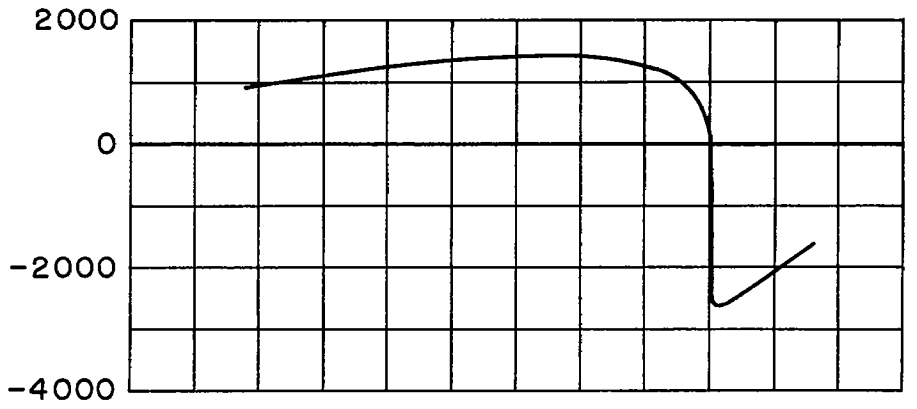

(a) Balancing loads.

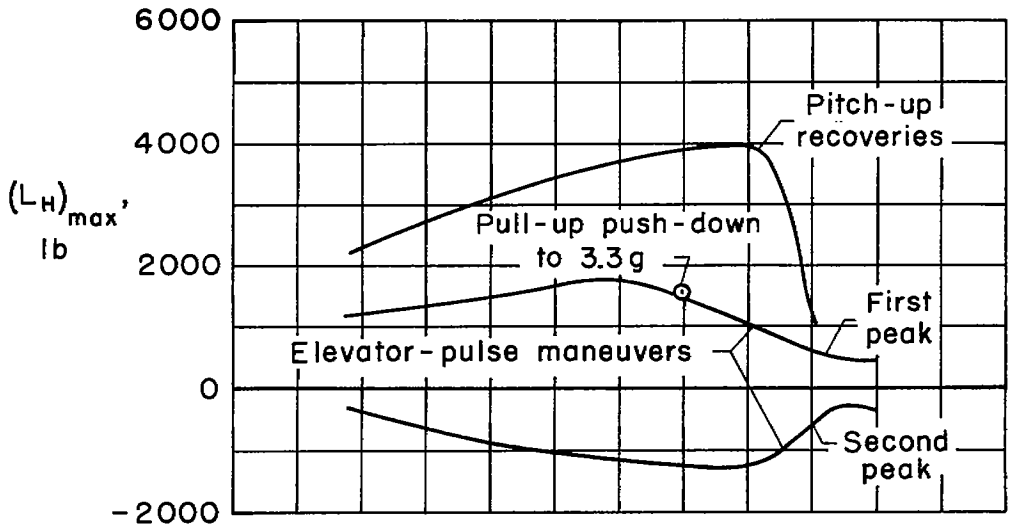

(b) Maneuvering loads.

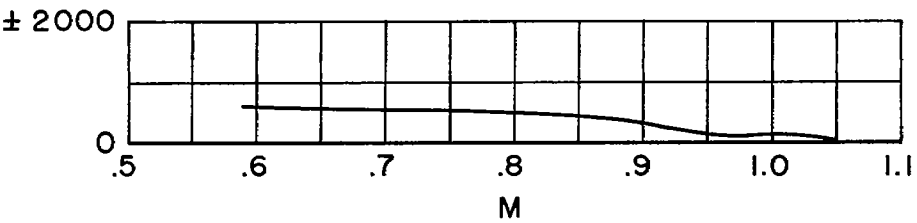

(c) Buffeting loads.

Figure 9.- Maximum balancing, maneuvering, and buffeting horizontal-tail loads obtained in various longitudinal maneuvers; pressure altitude, 35,000 feet.

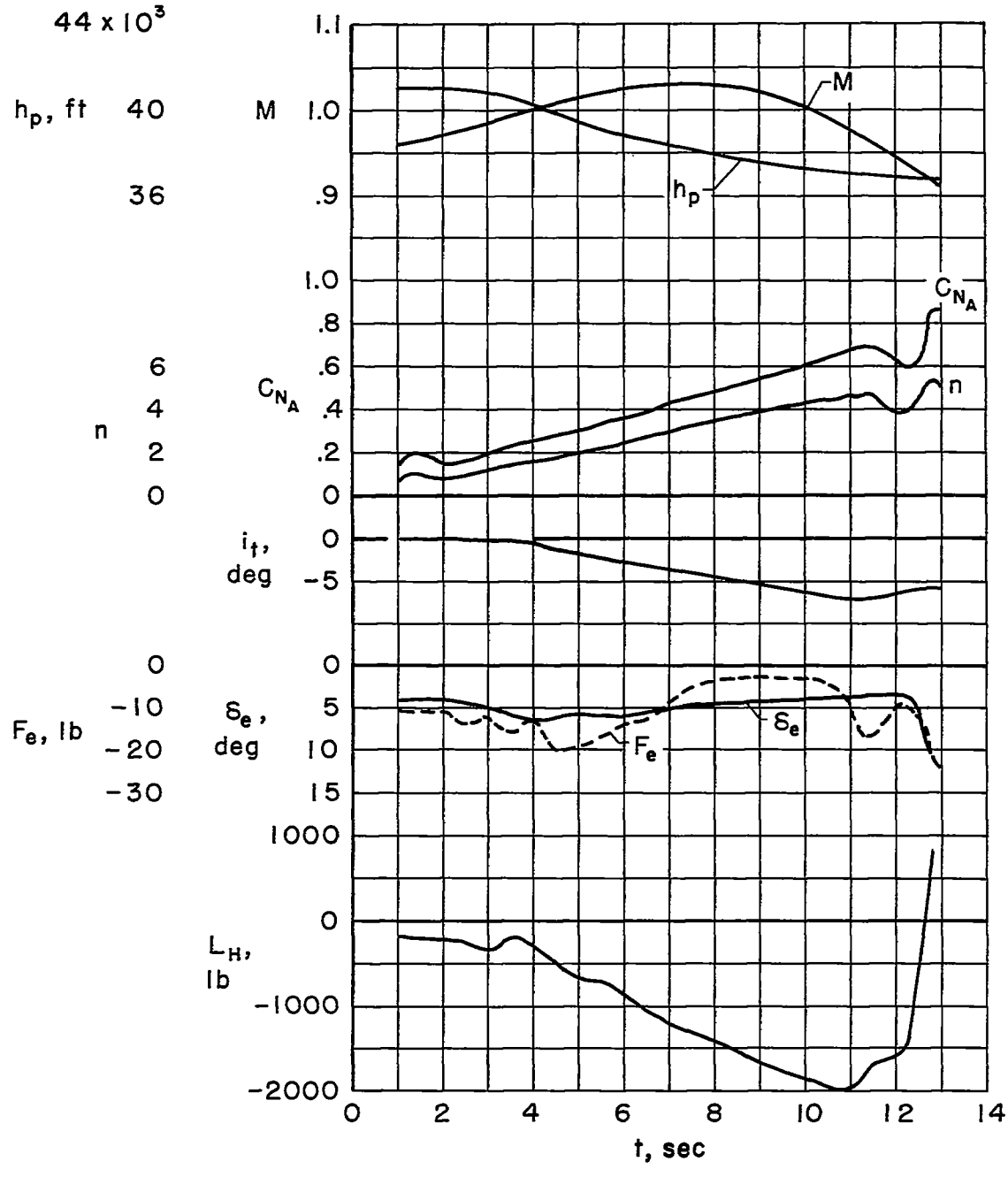

Figure 10.- Time history of a dive pull-out at high subsonic Mach numbers.

[redacted]

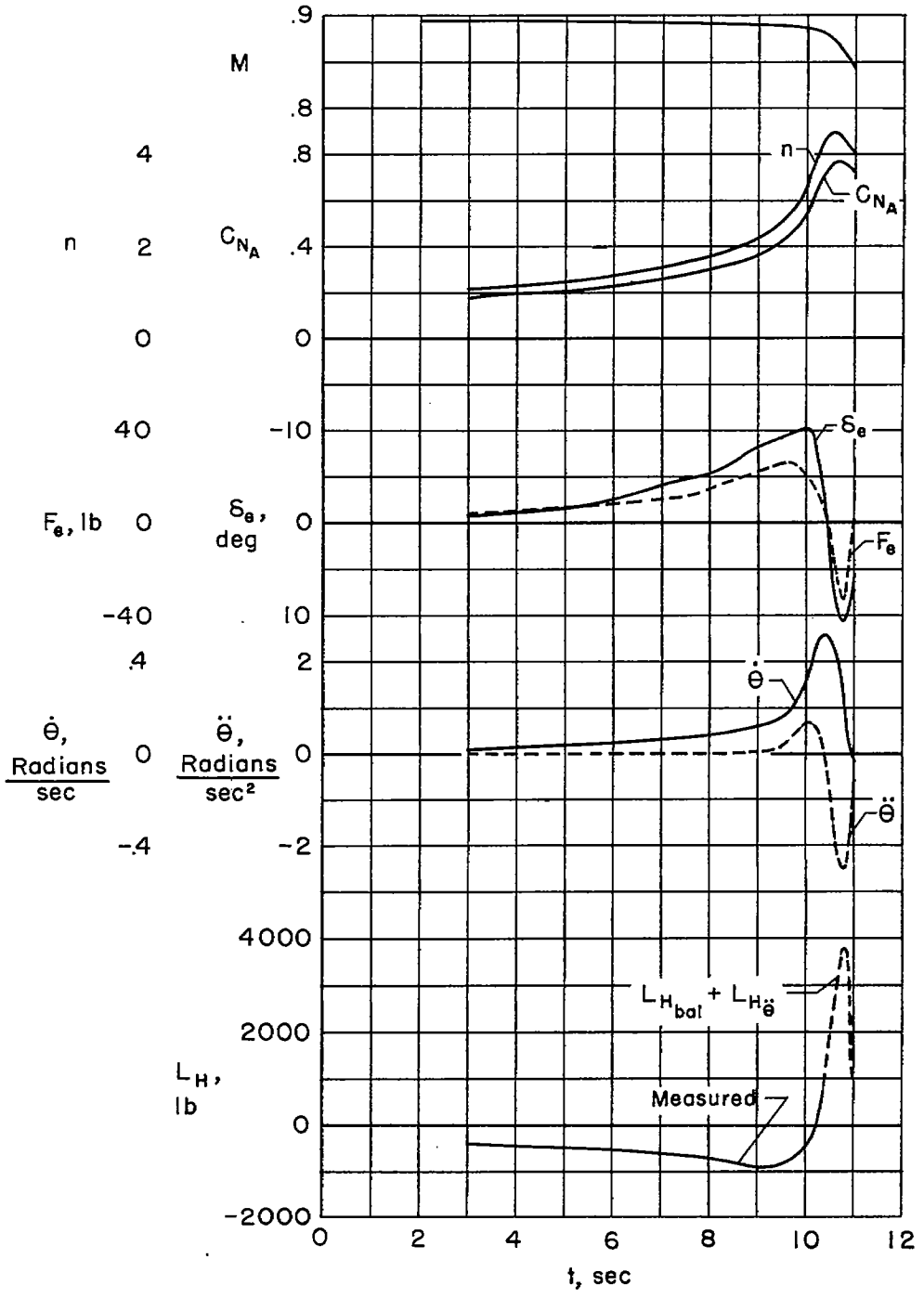

Figure 11.- Time history of a pitch-up at a Mach number of about 0.90; pressure altitude, 35,000 feet.

[redacted]

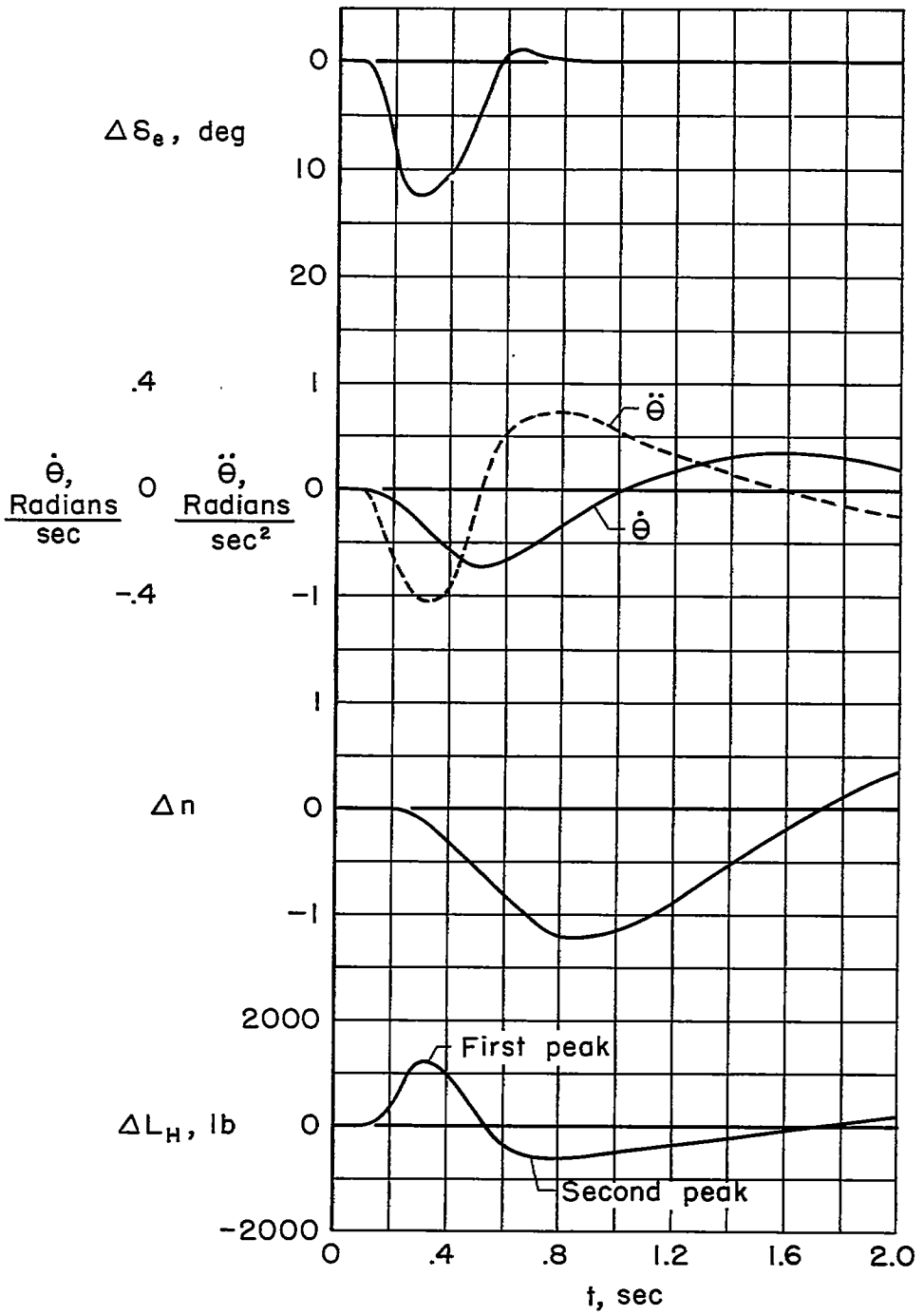

Figure 12.- Time history of an elevator-pulse maneuver at a Mach number of 0.59; pressure altitude, 35,000 feet.

[redacted]

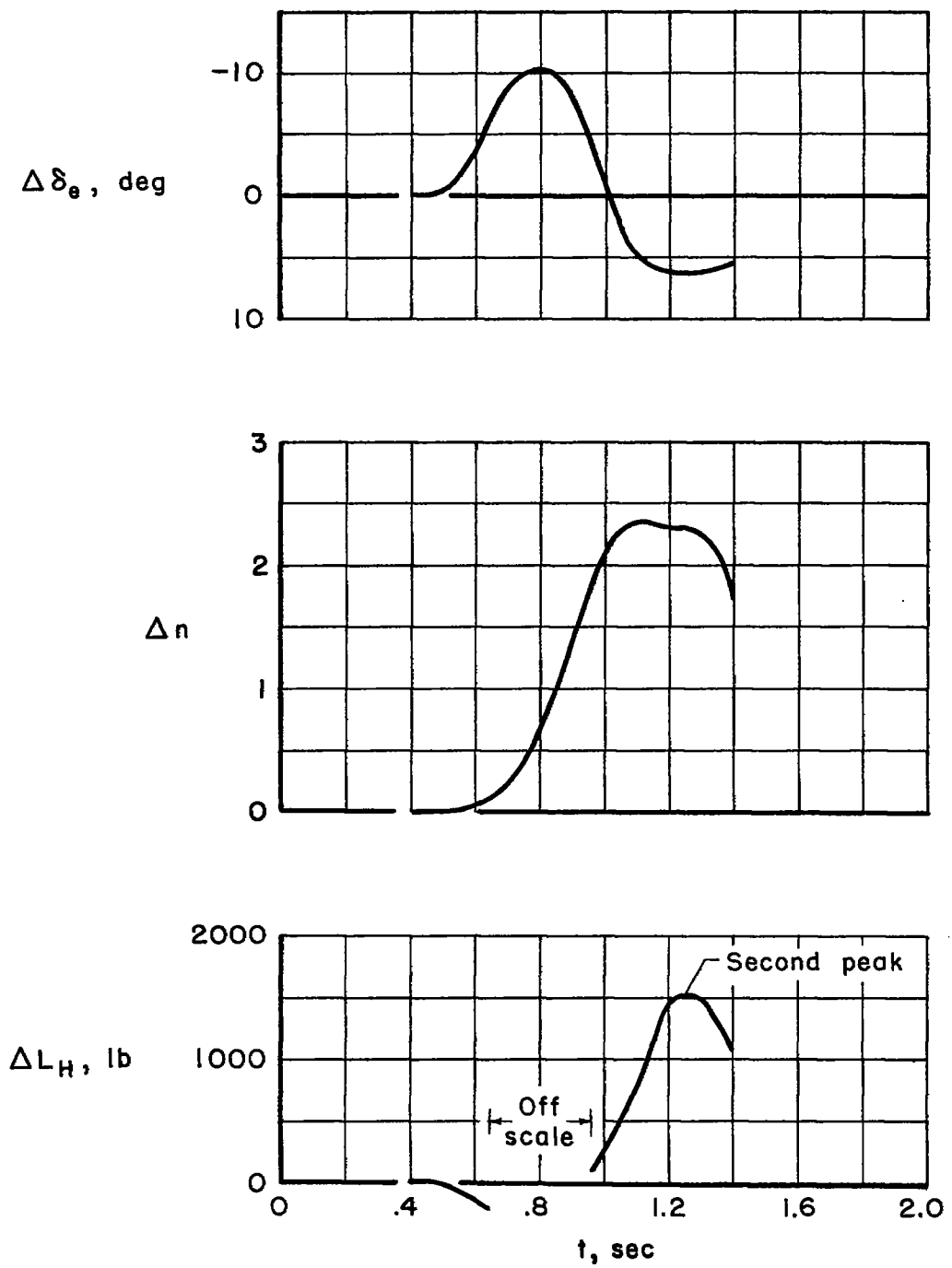

Figure 13.- Time history of a pull-up push-down maneuver at a Mach number of 0.85; pressure altitude, 35,000 feet.

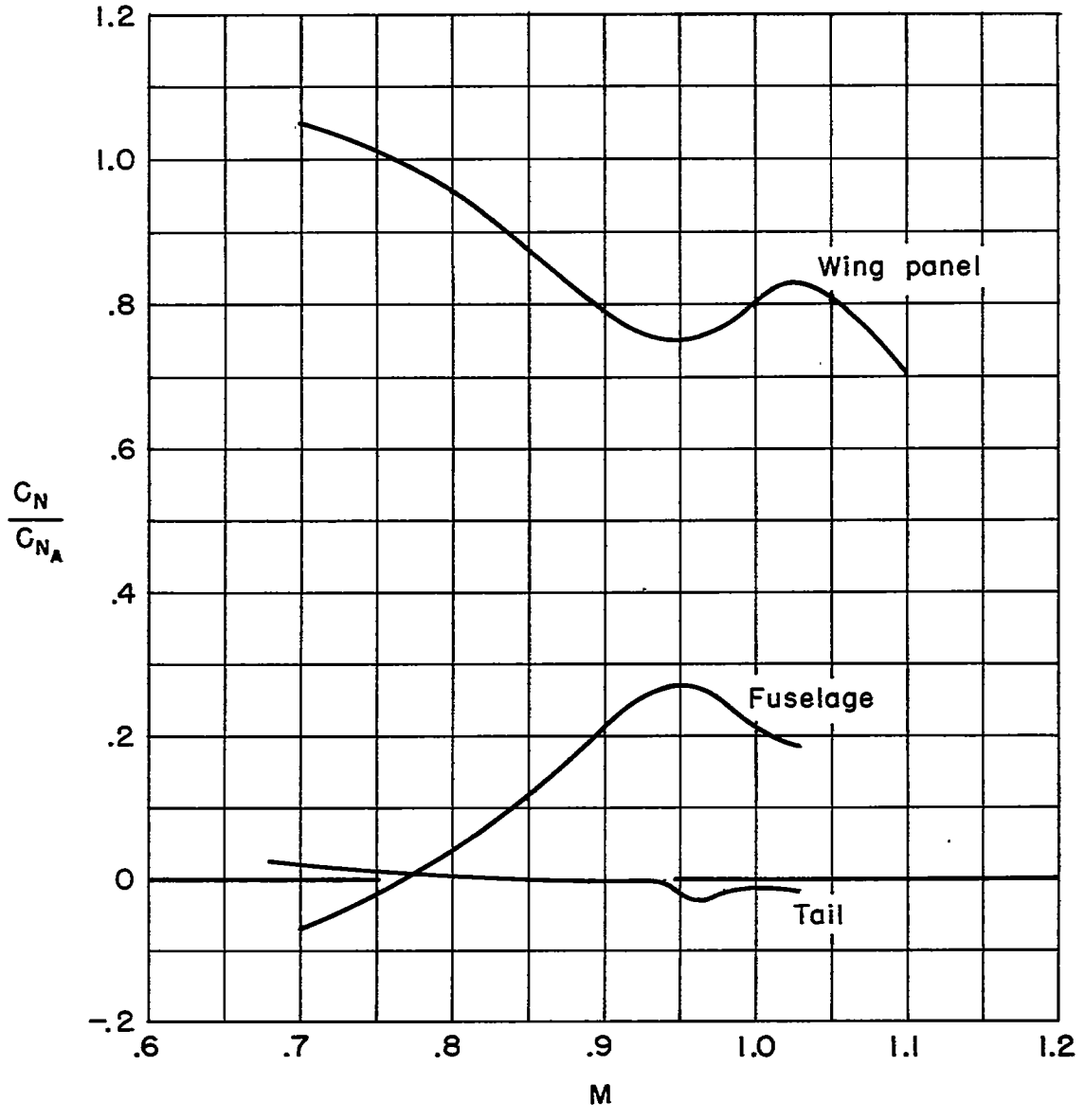

(a) $C_{N_A} = 0.2$

Figure 14.- Percentage of total load carried by the wing panel, fuselage, and horizontal tail at several values of airplane normal-force coefficient; pressure altitude, 35,000 feet.

[redacted]

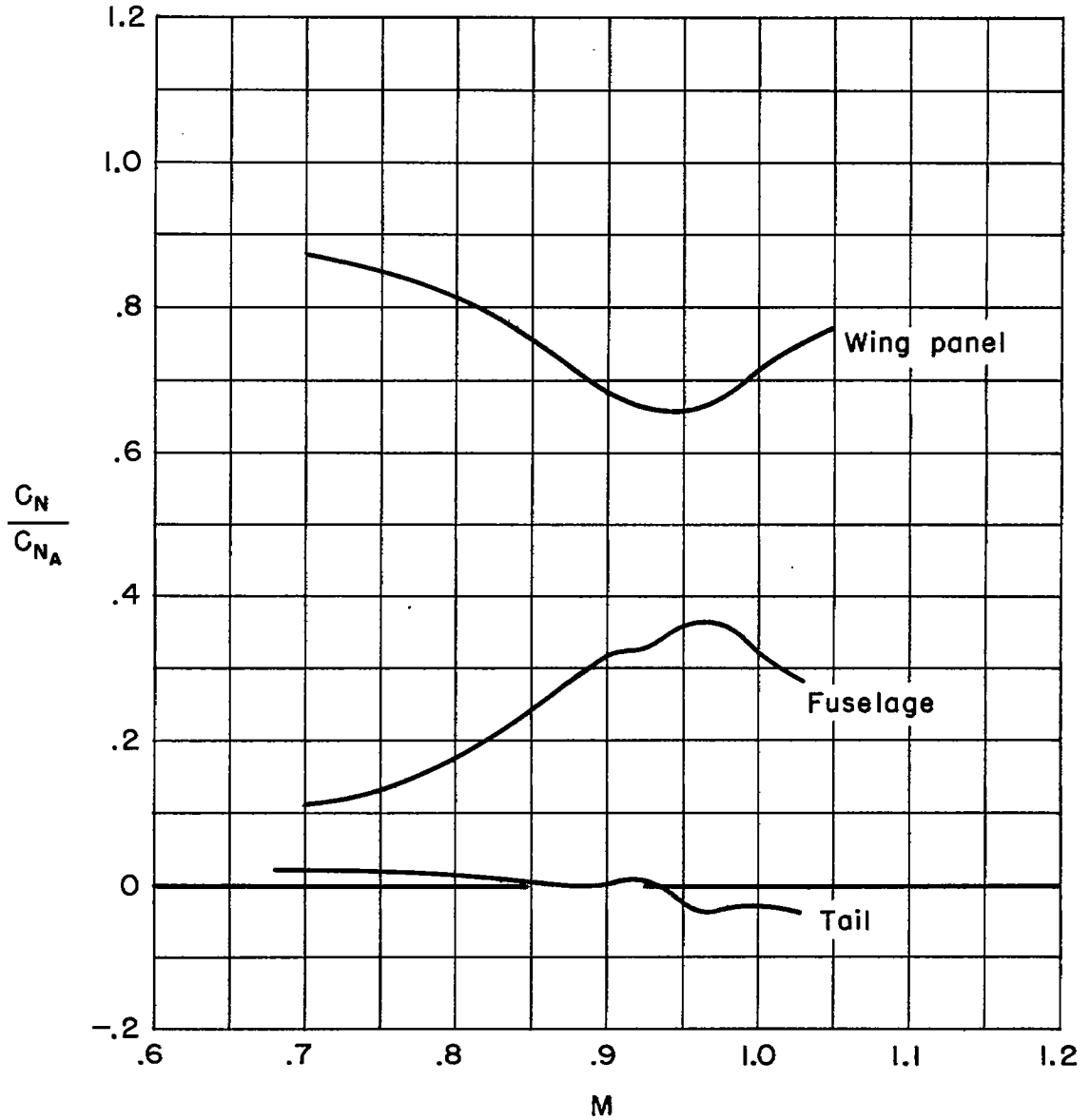

(b) $C_{N_A} = 0.4$

Figure 14.- Continued.

[redacted]

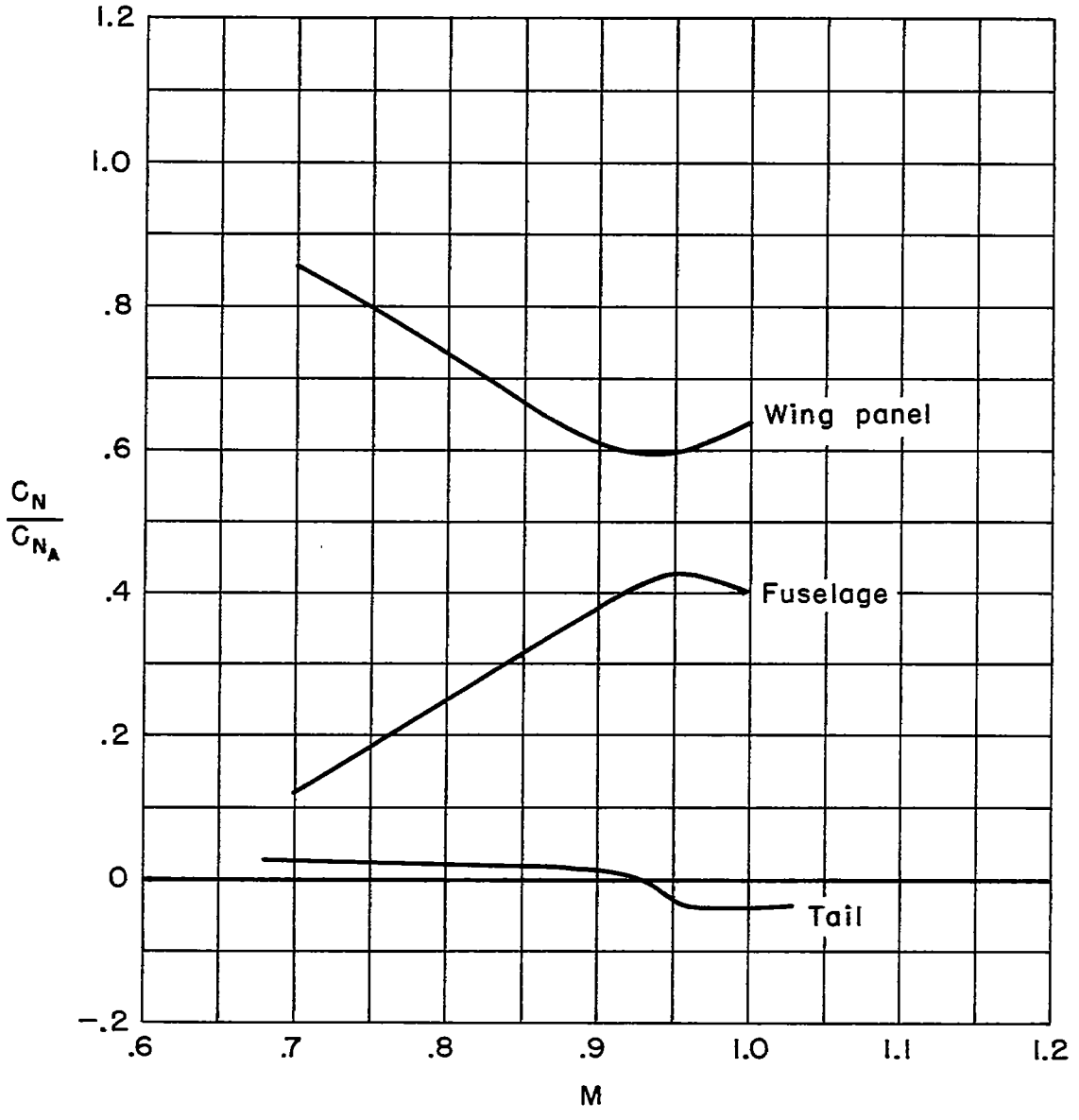

(c) $C_{N_A} = 0.6$

Figure 14.- Continued.

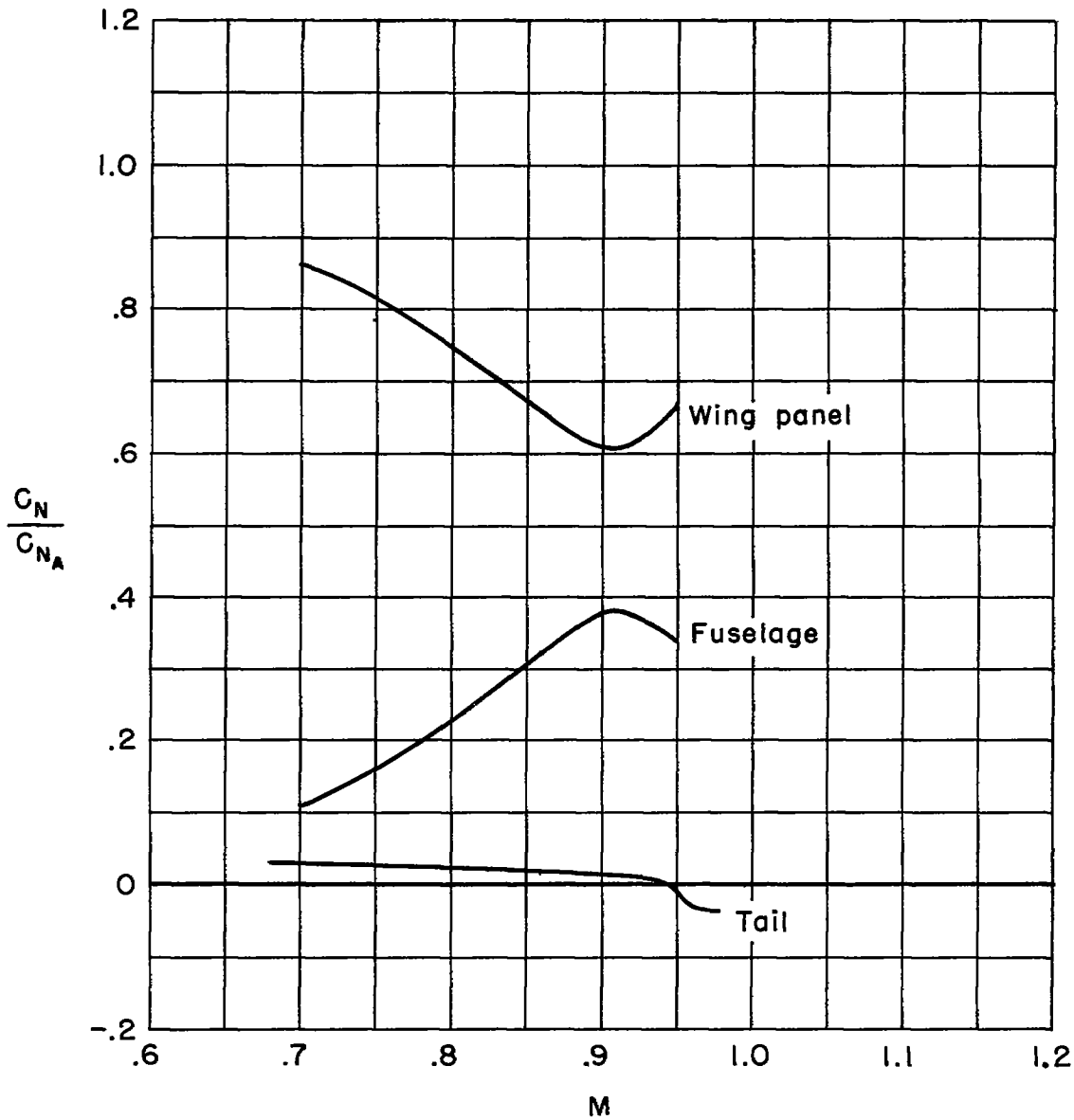

(d) $C_{N_A} = 0.8$

Figure 14.- Concluded.

[redacted]

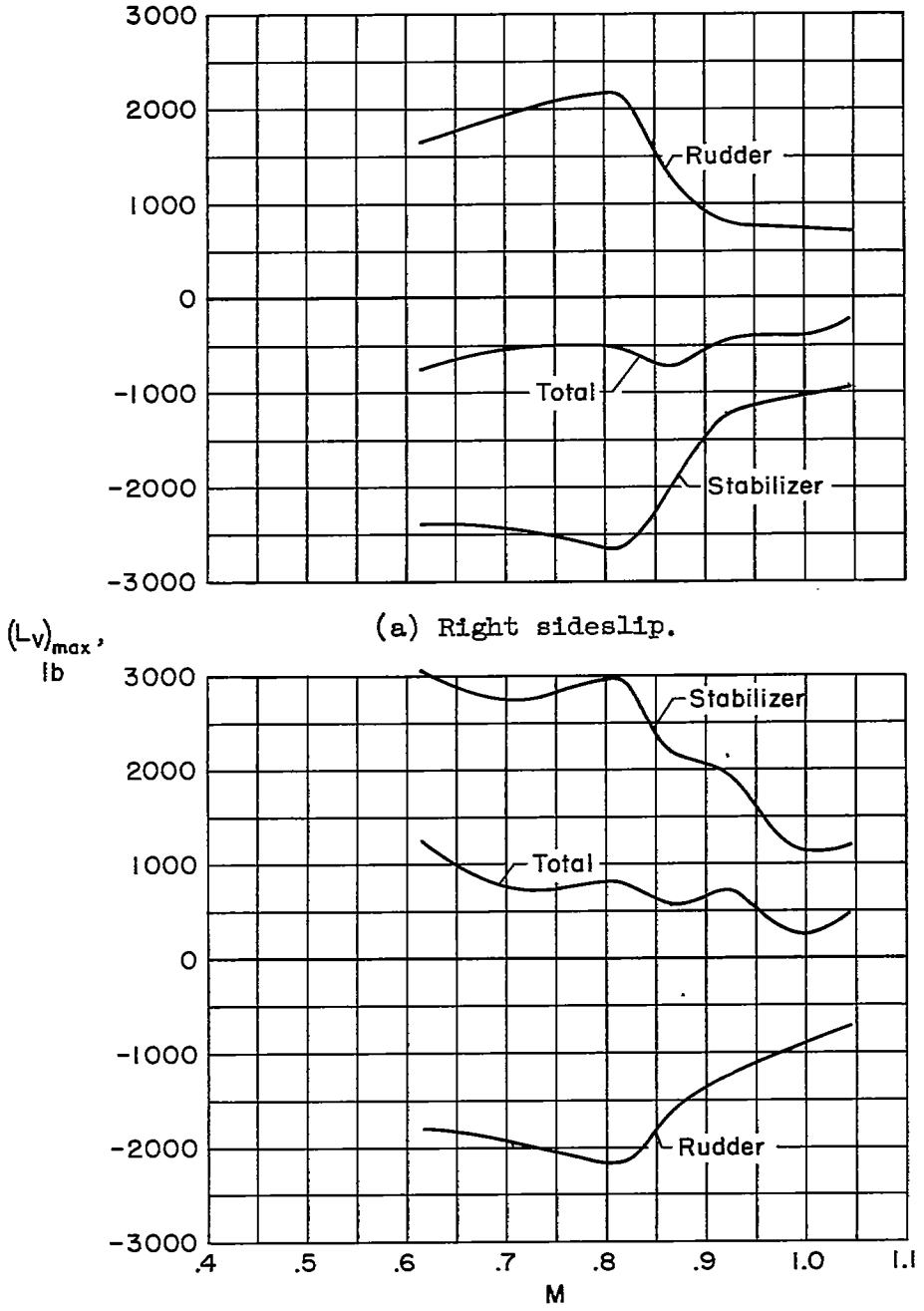

Figure 15.- Derived maximum balancing vertical-tail loads; pressure altitude, 35,000 feet.

[redacted]

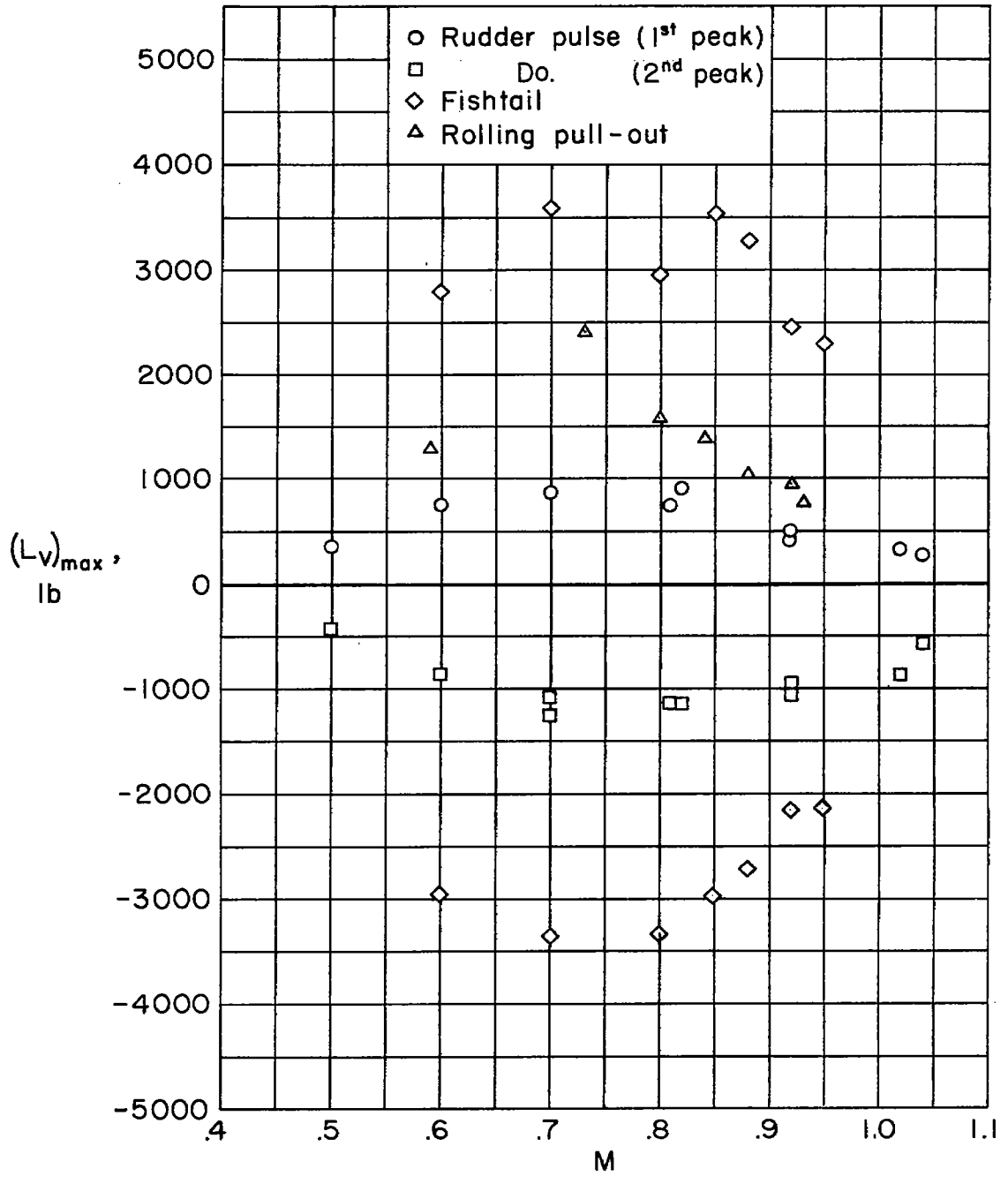

Figure 16.- Derived maximum maneuvering vertical-tail loads; pressure altitude, 35,000 feet.

[redacted]

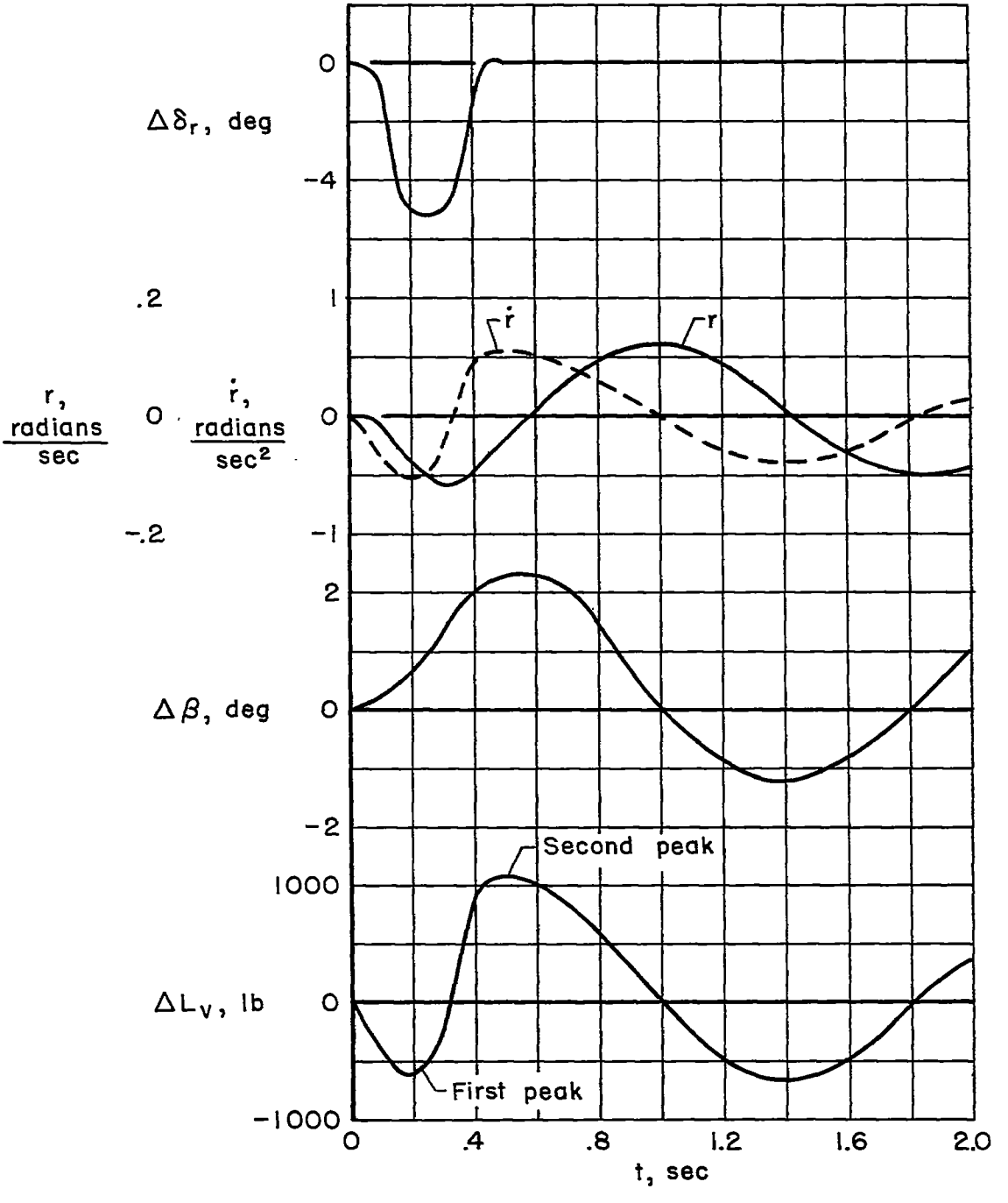

Figure 17.- Time history of a rudder-pulse maneuver at a Mach number of 0.81; pressure altitude, 35,000 feet.

[redacted]

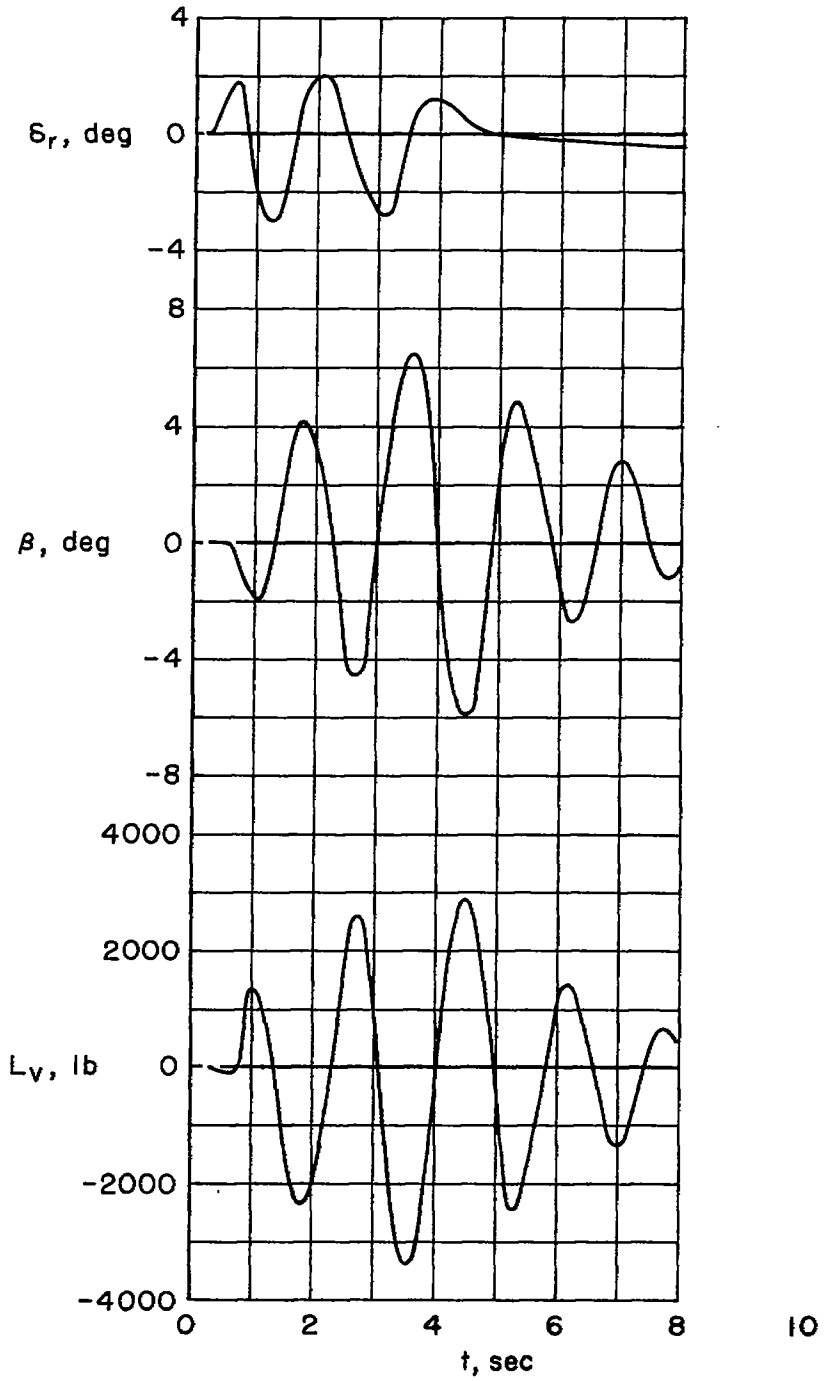

Figure 18.- Time history of a fishtail maneuver at a Mach number of 0.80; pressure altitude, 35,000 feet.

[redacted]

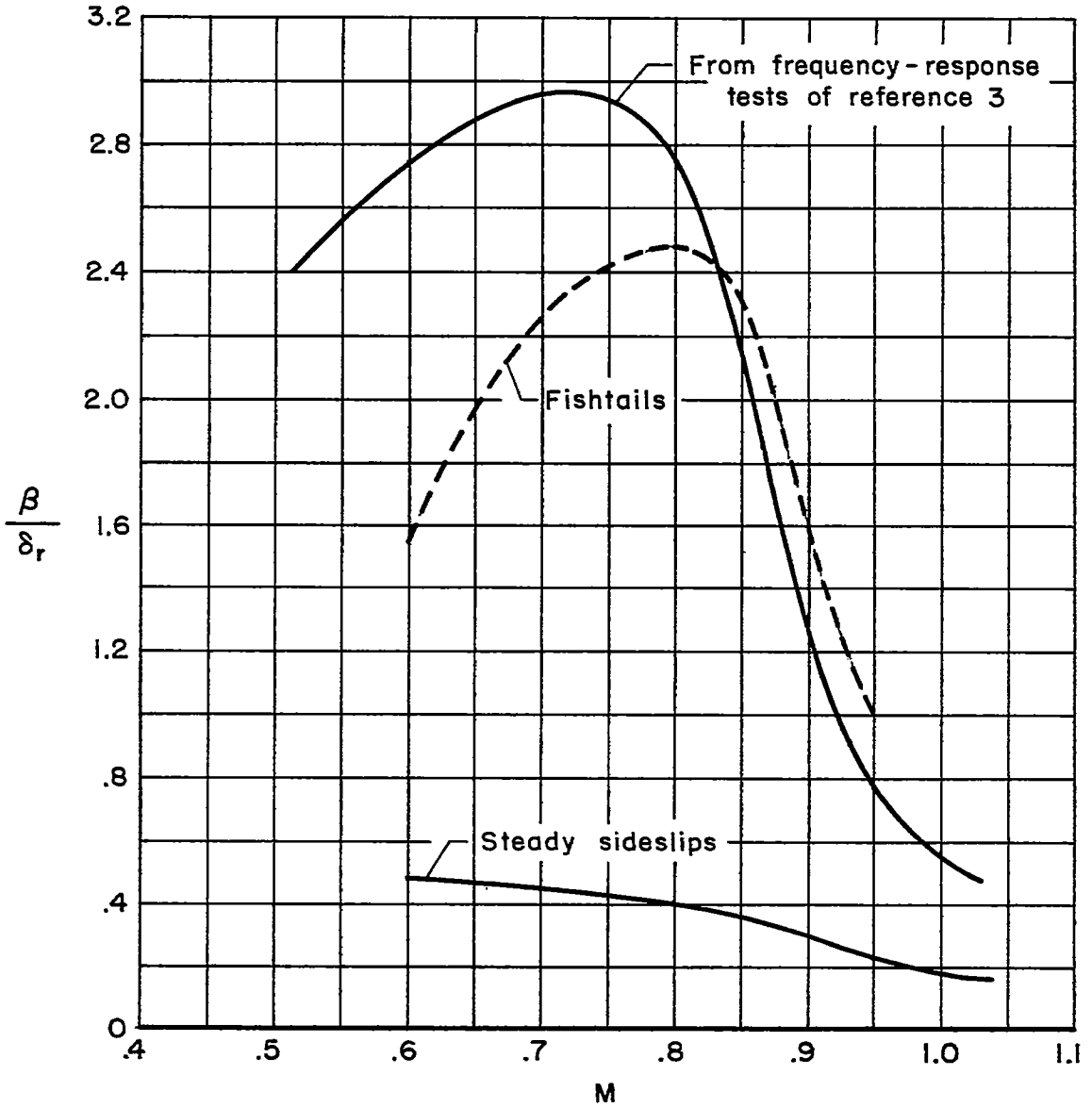

Figure 19.- Variation with Mach number of the ratio of sideslip angle to rudder angle from frequency-response analysis and from fishtail and steady-sideslip maneuvers.

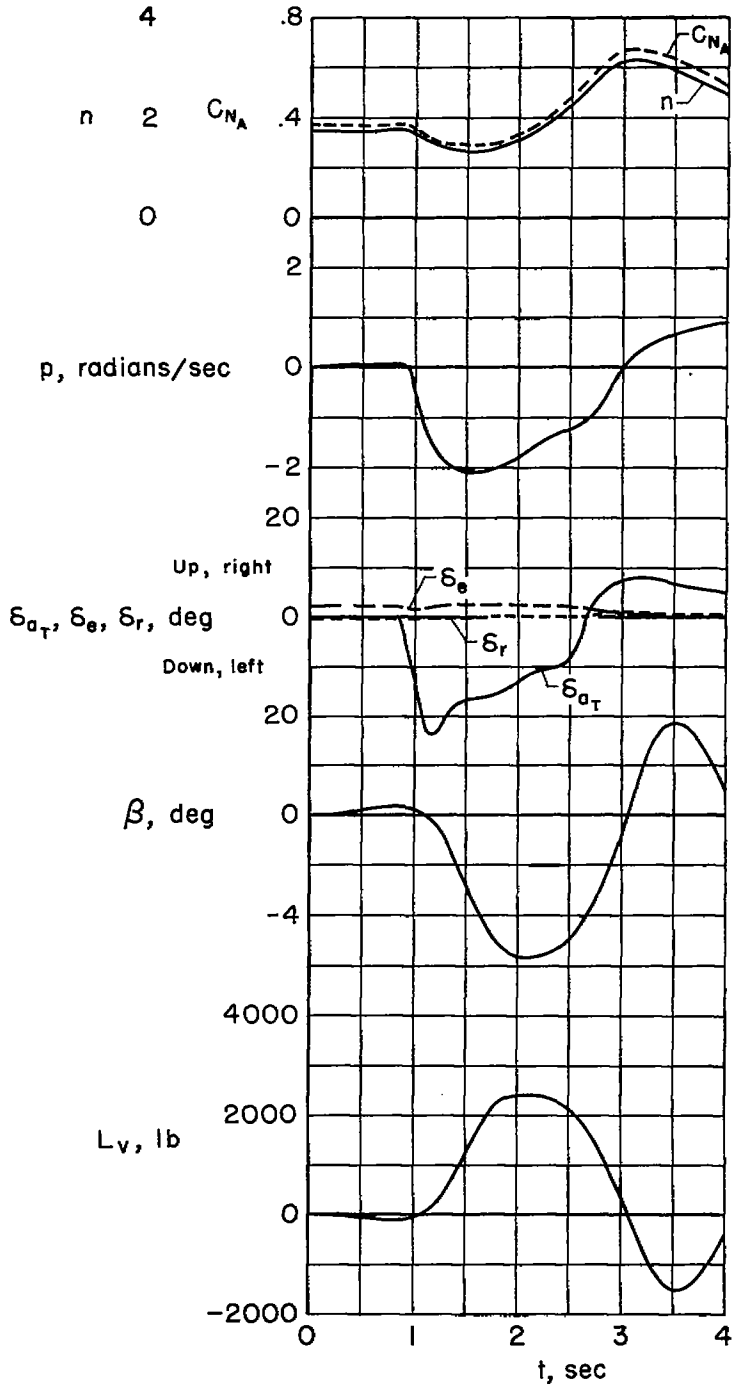

Figure 20.- Time history of a rolling pull-out maneuver below the pitch-up boundary at a Mach number of 0.73; pressure altitude, 35,000 feet.

[redacted]

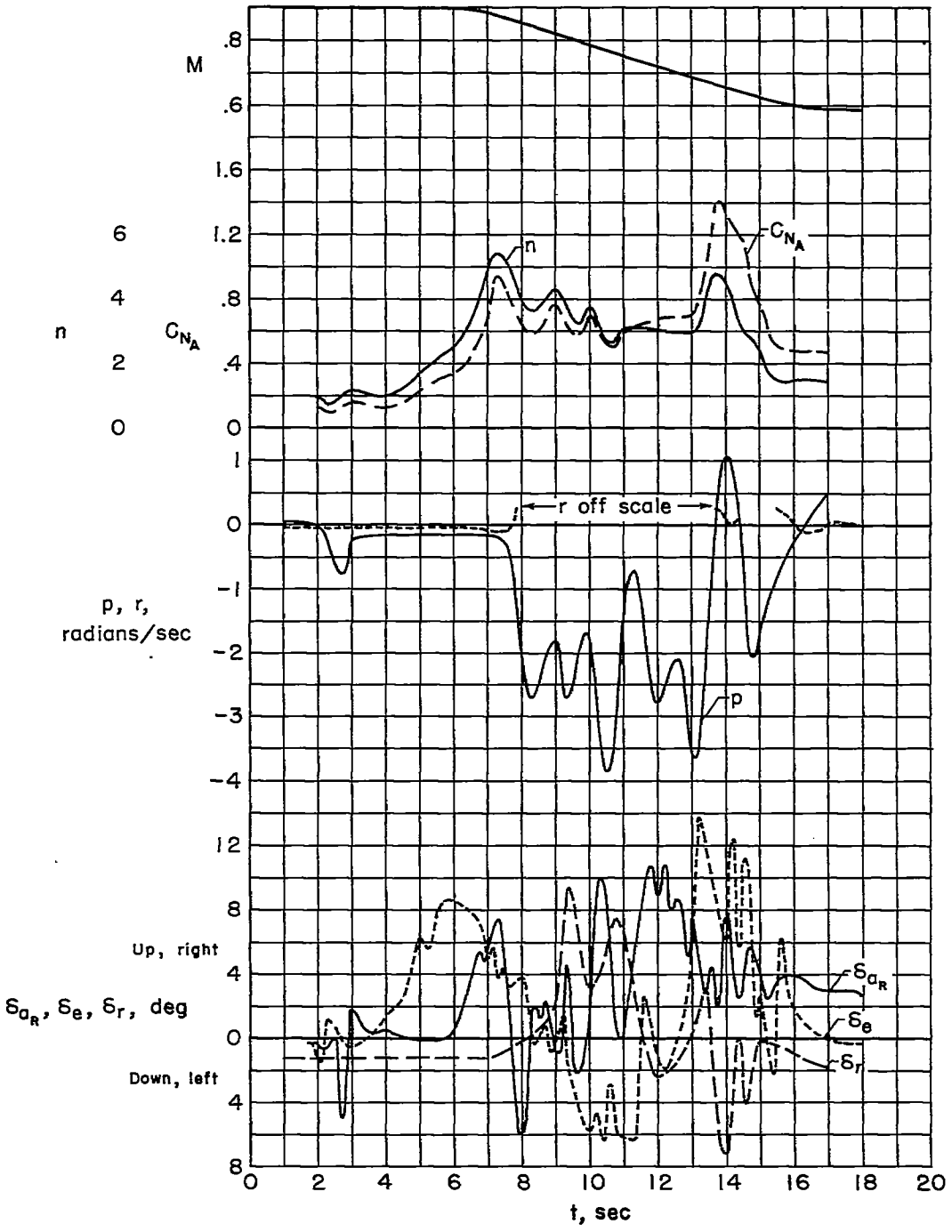

Figure 21.- Time history of a rolling pull-out maneuver performed at load factors above the pitch-up boundary; pressure altitude, 35,000 feet.

[redacted]

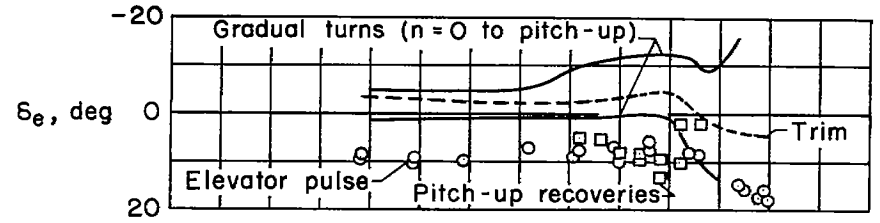

(a) Elevator angles.

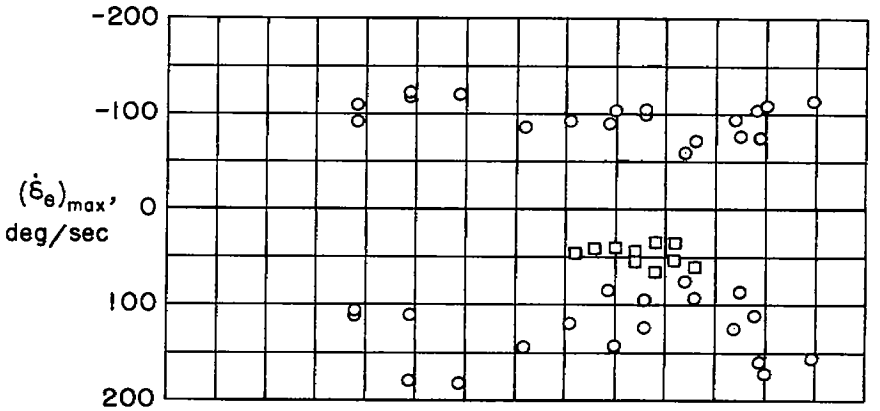

(b) Maximum elevator rates.

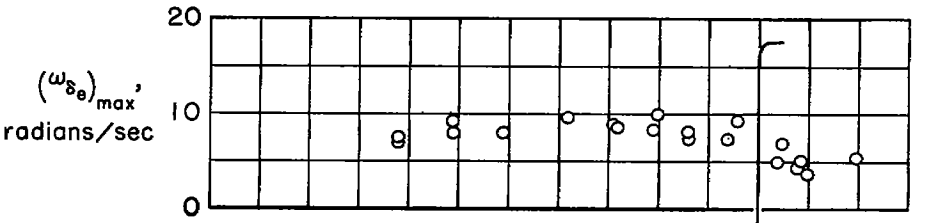

(c) Maximum elevator frequencies.

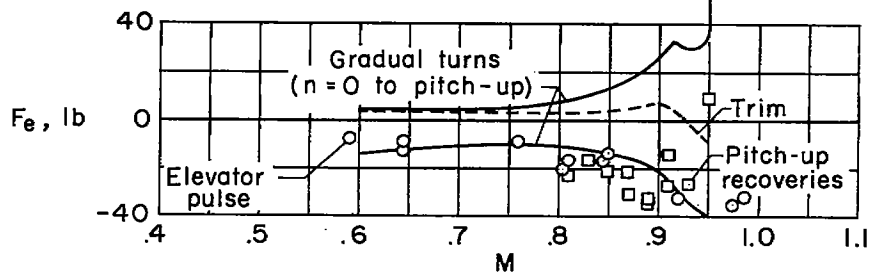

(d) Elevator stick forces.

Figure 22.- Use of controls in various longitudinal maneuvers; pressure altitude, 35,000 feet.

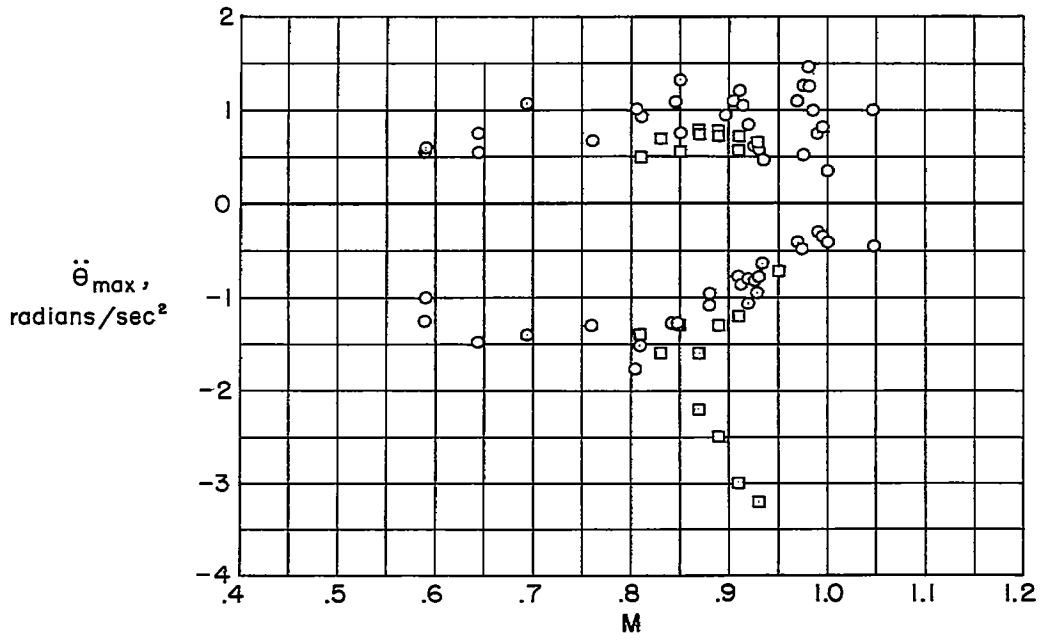

(a) Mach number.

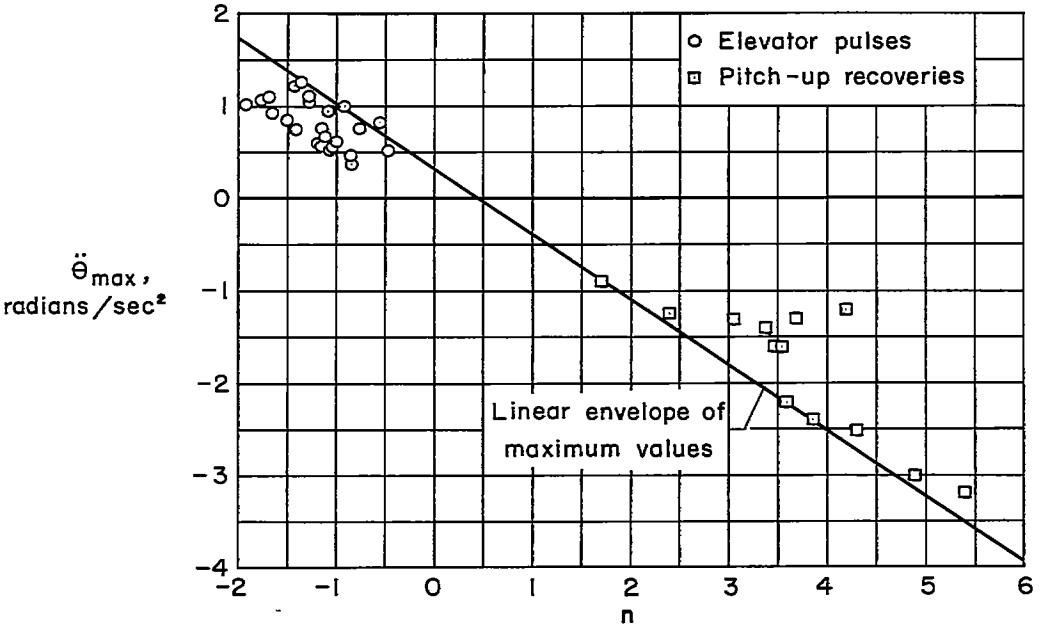

(b) Load factor.

Figure 23.- Maximum pitching accelerations developed in various longitudinal maneuvers; pressure altitude, 35,000 feet.

[redacted]

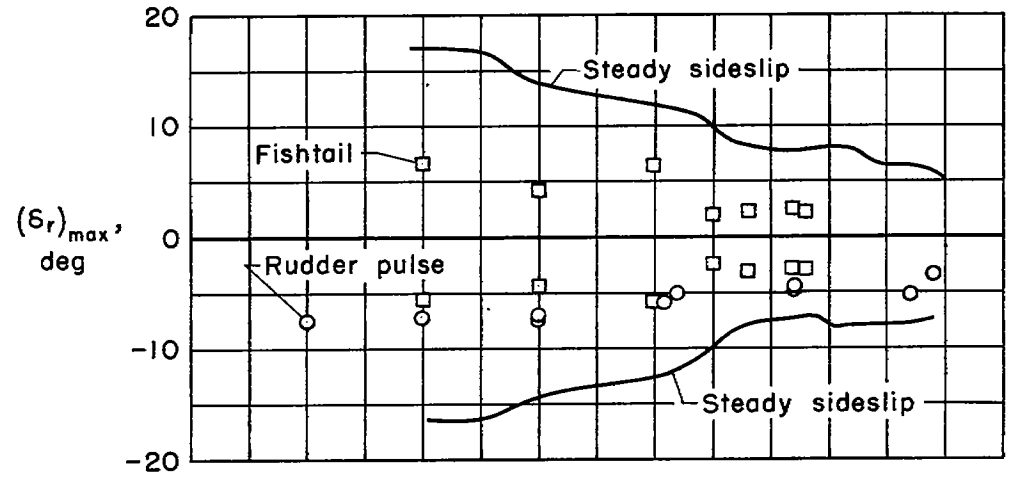

(a) Maximum rudder angles.

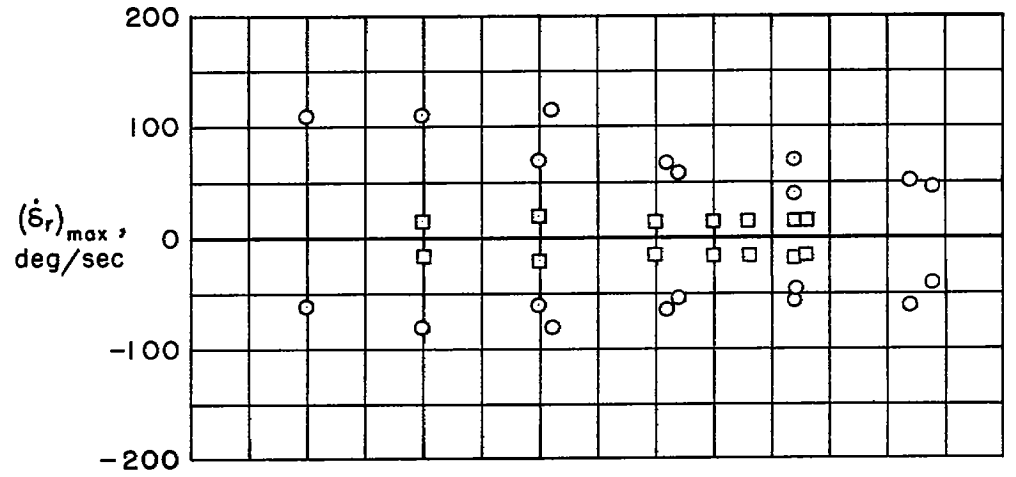

(b) Maximum rudder rates.

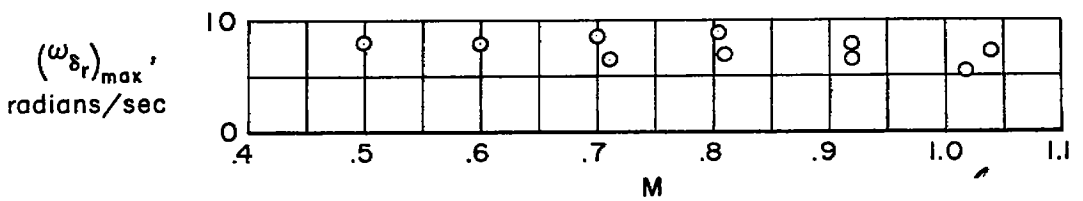

(c) Maximum rudder frequencies.

Figure 24.- The use of controls in various directional maneuvers; pressure altitude, 35,000 feet.

[redacted]

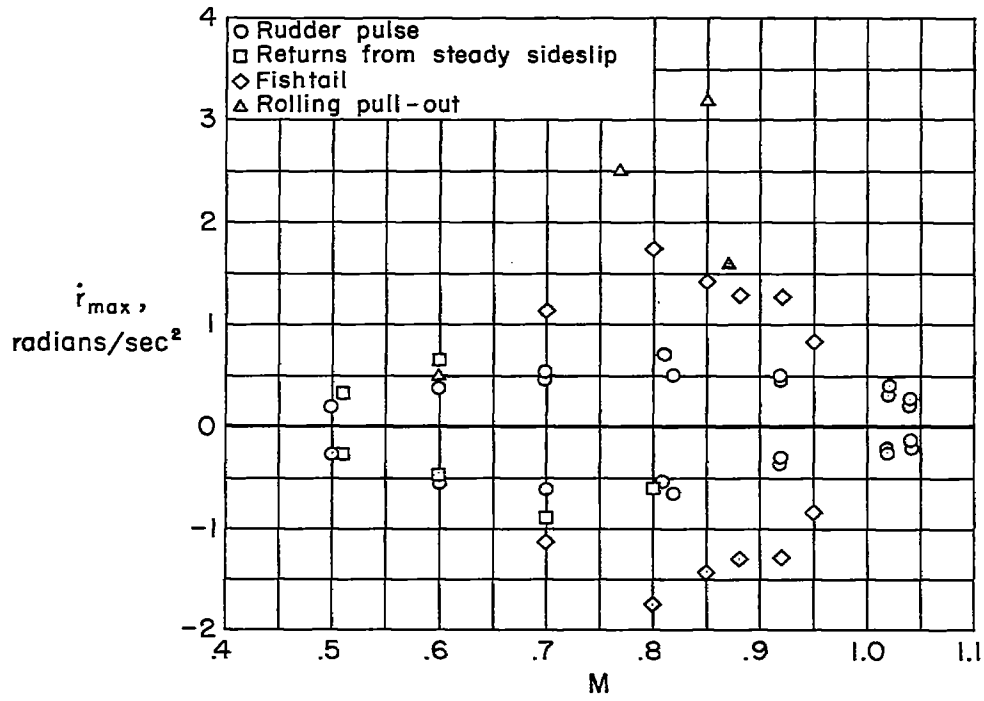

(a) Mach number.

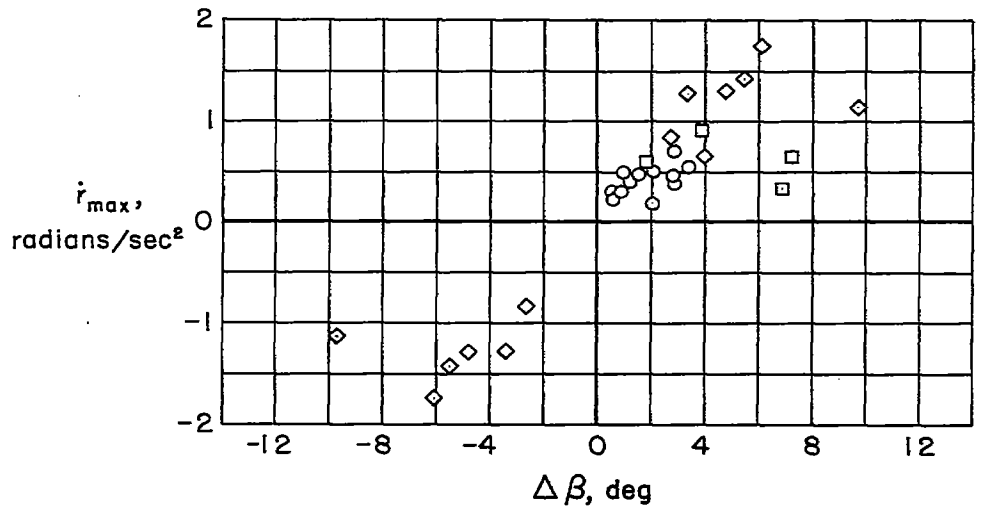

(b) Sideslip angle, $\Delta\beta$, deg.

Figure 25.- Maximum yawing accelerations attained in directional and rolling pull-out maneuvers; pressure altitude, 35,000 feet.

[redacted]

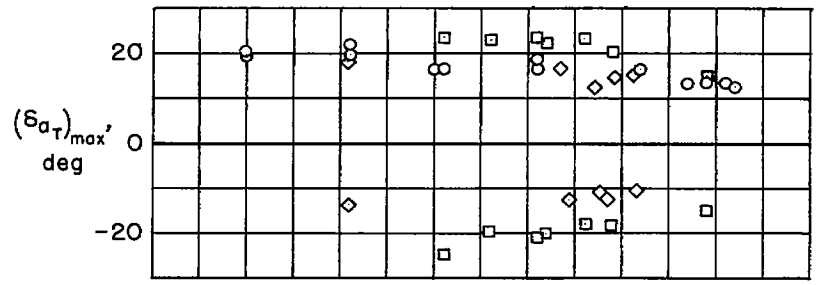

(a) Maximum total aileron angles.

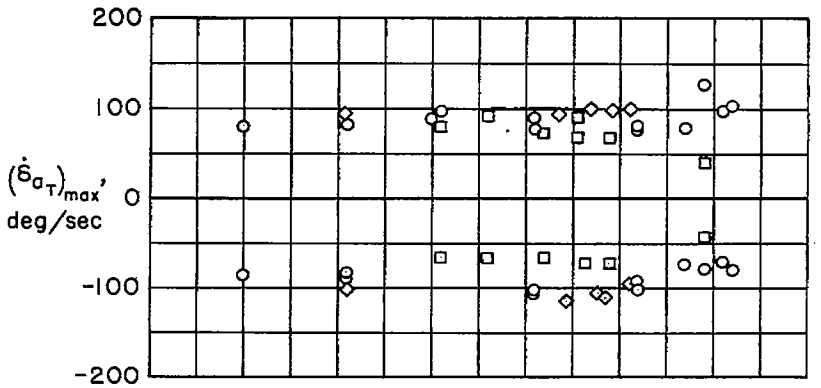

(b) Maximum total aileron rates.

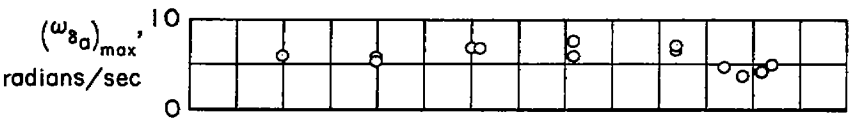

(c) Maximum total aileron frequencies.

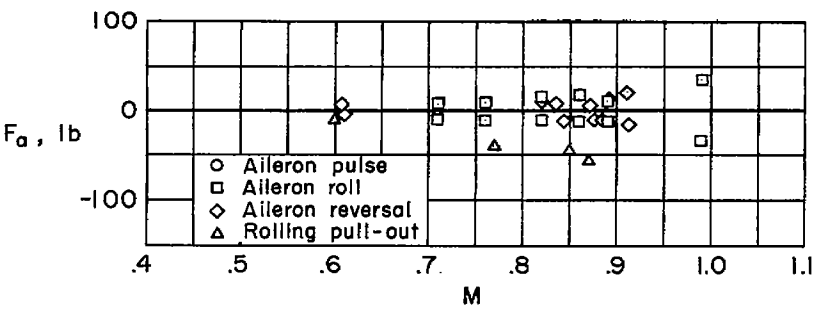

(d) Maximum aileron stick forces.

Figure 26.- Use of controls in various lateral maneuvers; pressure altitude, 35,000 feet.

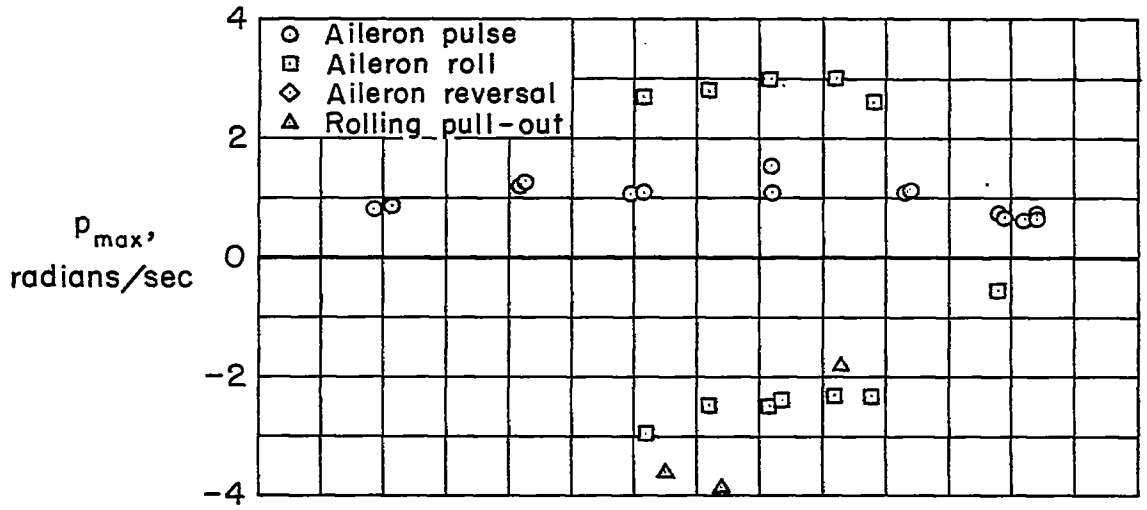

(a) Maximum rolling velocities.

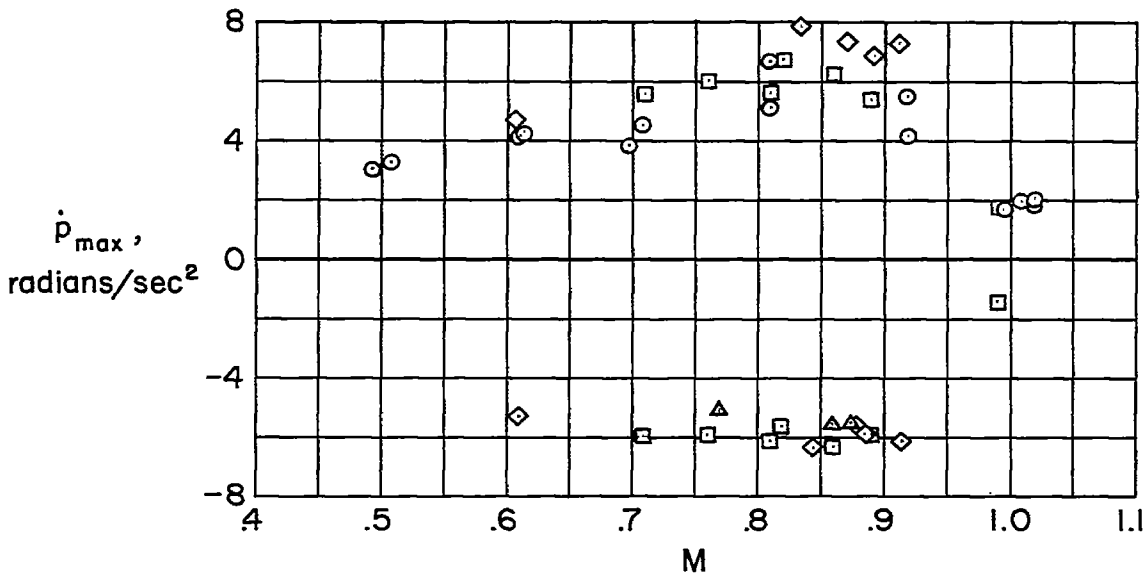

(b) Maximum rolling accelerations.

Figure 27.- Maximum rolling velocities and rolling accelerations developed in various lateral maneuvers; pressure altitude, 35,000 feet.

[redacted]